

1 **The *Drosophila* TART transposon manipulates the piRNA pathway as a counter-defense**
2 **strategy to limit host silencing**

3
4 Christopher E. Ellison, Meenakshi S. Kagda*, Weihuan Cao
5 Department of Genetics, Human Genetics Institute of New Jersey, Rutgers, The State University of
6 New Jersey, Piscataway, New Jersey

7
8 *Current Affiliation: Department of Genetics, Stanford University, Stanford, California

9
10 Corresponding author:
11 Christopher E. Ellison
12 chris.ellison@rutgers.edu

13
14
15 **Short title: *Drosophila* transposon counter-defense**
16
17
18
19
20
21
22
23
24
25
26
27
28
29
30
31
32
33
34
35
36
37
38
39
40
41
42
43
44
45
46
47
48
49
50
51
52
53
54

1 Abstract

2 Co-evolution between transposable elements (TEs) and their hosts can be antagonistic, where TEs
3 evolve to avoid silencing and the host responds by reestablishing TE suppression, or mutualistic, where
4 TEs are co-opted to benefit their host. The *TART-A* TE functions as an important component of
5 *Drosophila* telomeres, but has also reportedly inserted into the *D. melanogaster* nuclear export factor
6 gene *nxf2*. We find that, rather than inserting into *nxf2*, *TART-A* has actually captured a portion of *nxf2*
7 sequence. We show that Nxf2 is involved in suppressing *TART-A* activity via the piRNA pathway and
8 that *TART-A* produces abundant piRNAs, some of which are antisense to the *nxf2* transcript. We
9 propose that capturing *nxf2* sequence allowed *TART-A* to target the *nxf2* gene for piRNA-mediated
10 repression and that these two elements are engaged in antagonistic co-evolution despite the fact that
11 *TART-A* is serving a critical role for its host genome.

13 Introduction

14 Transposable elements (TEs) must replicate faster than their host to avoid extinction. The vast majority
15 of new TE insertions derived from this replicative activity are deleterious to their host: they can disrupt
16 and/or silence protein-coding genes and lead to chromosome rearrangements (Y. C. Lee, 2015; Y. C.
17 G. Lee & Karpen, 2017; Petrov, Fiston-Lavier, Lipatov, Lenkov, & Gonzalez, 2011). In response to the
18 mutational burden imposed by TEs, TE hosts have evolved elaborate genome surveillance
19 mechanisms to identify and target TEs for suppression. One of the most well-known genome defense
20 pathways in metazoan species involves the production of piwi-interacting small RNAs, also known as
21 piRNAs (Brennecke et al., 2007). PiRNA precursors are produced from so-called piRNA clusters, which
22 are located in heterochromatic regions of the genome and contain fragments of many families of TEs,
23 whose insertions have accumulated in these regions. These precursors are processed into primary
24 piRNAs, which use sequence homology to guide piwi-proteins to complementary transcripts produced
25 by active transposable elements (Brennecke et al., 2007; Gunawardane et al., 2007). Piwi proteins
26 induce transcriptional silencing through cleavage of the TE transcript. The sense-strand cleavage
27 product of the TE transcript can then aid in processing piRNA precursors through a process known as
28 the ping-pong cycle, which amplifies the silencing signal (Brennecke et al., 2007; Gunawardane et al.,
29 2007). Alternatively, the cleaved transcript can be processed by the endonuclease Zucchini into
30 additional “phased” piRNAs starting from the cleavage site and proceeding in the 3’ direction (Han,
31 Wang, Li, Weng, & Zamore, 2015; Mohn, Handler, & Brennecke, 2015).

32 In addition to piRNAs, various other host mechanisms have evolved to target TEs (Cam, Noma, Ebina,
33 Levin, & Grewal, 2008; Esnault et al., 2005; Satyaki et al., 2014; Thomas & Schneider,
34 2011)(mammalian systems reviewed in (Molaro & Malik, 2016)). Despite these multiple layers of
35 genome surveillance, active TEs are found in the genomes of most organisms. The ubiquity of active
36 TEs suggests that host silencing mechanisms are not completely effective, possibly because the TE
37 and its host genome are involved in an evolutionary “arms race” where TEs are continuously evolving
38 novel means to avoid host silencing and the host genome is constantly reestablishing TE suppression
39 (Parhad & Theurkauf, 2019). On the host side, many TE silencing components have been shown to be
40 evolving rapidly under positive selection (Crysnanto & Obbard, 2019; Helleu & Levine, 2018; Jacobs et
41 al., 2014; Kelleher, Edelman, & Barbash, 2012; Kolaczkowski, Hupalo, & Kern, 2011; Levine, Vander
42 Wende, Hsieh, Baker, & Malik, 2016; Obbard, Jiggins, Bradshaw, & Little, 2011; Obbard, Jiggins,
43 Halligan, & Little, 2006; Simkin, Wong, Poh, Theurkauf, & Jensen, 2013), in agreement with on-going
44 host-TE conflict. On the transposon side, a TE can mount a counter-defense by silencing or blocking
45 host factors (Fu et al., 2013; McCue, Nuthikattu, & Slotkin, 2013; Nosaka et al., 2012) or simply evade
46 host silencing by replicating in permissive cells (L. Wang, Dou, Moon, Tan, & Zhang, 2018) or cloaking
47 themselves in virus-like particles (Mari-Ordonez et al., 2013). However, there are surprisingly few
48 examples of any of these strategies (Cosby, Chang, & Feschotte, 2019). In fact, there is some evidence
49 that, rather than an evolutionary arms race, the rapid evolution of host silencing genes is related to
50 avoiding gene silencing due to off-target effects (i.e. piRNA autoimmunity (Blumenstiel, Erwin, &
51 Hemmer, 2016; Luyang Wang, Barbash, & Kelleher, 2019)) and/or co-evolution with viruses (reviewed
52 in (Cosby et al., 2019)).

53 While there are currently only a few examples of TE counter-defense strategies, there are many
54 examples of TEs being co-opted by their host genome for its own advantage (see reviews (Bohne,

1 Brunet, Galiana-Arnoux, Schultheis, & Voff, 2008; Chuong, Elde, & Feschotte, 2017; Cosby et al.,
2 2019; Feschotte, 2008; Voff, 2006)). TEs can disperse regulatory sequences across the genome,
3 which allows them to rewire gene regulatory networks. Such rewiring phenomena have been implicated
4 in a variety of evolutionary innovations from pregnancy to dosage compensation (Chuong, Elde, &
5 Feschotte, 2016; Chuong, Rumi, Soares, & Baker, 2013; Dunn-Fletcher et al., 2018; C. Ellison &
6 Bachtrog, 2019; C. E. Ellison & Bachtrog, 2013; Fuentes, Swigut, & Wysocka, 2018; Lynch, Leclerc,
7 May, & Wagner, 2011; Lynch et al., 2015; Notwell, Chung, Heavner, & Bejerano, 2015; Pontis et al.,
8 2019). TEs are also an important source of host genes and noncoding RNAs (Joly-Lopez & Bureau,
9 2018; Kapusta et al., 2013). Hundreds of genes in species ranging from mammals to plants have been
10 acquired from transposons (Bohne et al., 2008; Joly-Lopez, Hoen, Blanchette, & Bureau, 2016; Voff,
11 2006). Finally, TEs can act as structural components of the genome. There is evidence that TEs may
12 play a role in centromere specification in a variety of species (Chang et al., 2019; Chueh, Northrop,
13 Brettingham-Moore, Choo, & Wong, 2009; Klein & O'Neill, 2018), and in *Drosophila*, which lacks
14 telomerase, specific TEs serve as telomeres by replicating to chromosome ends (Levis, Ganesan,
15 Houtchens, Tolar, & Sheen, 1993; Traverse & Pardue, 1988).

16 In *Drosophila melanogaster*, three related non-LTR retrotransposons occupy the telomeres: *HeT-A*,
17 *TAHRE*, and *TART*, which are often abbreviated as HTT elements (Abad et al., 2004b; Biessmann et
18 al., 1992; Levis et al., 1993; Sheen & Levis, 1994). These elements belong to the Jockey clade of Long
19 Interspersed Nuclear Elements (LINEs), which contain open reading frames for gag (ORF1) and an
20 endonuclease/reverse transcriptase protein (ORF2, lost in *HeT-A*) (Malik, Burke, & Eickbush, 1999;
21 Villasante et al., 2007). These elements form head-to-tail arrays at the chromosome ends and their
22 replication solves the chromosome “end-shortening” problem without the need for telomerase
23 (Biessmann & Mason, 1997).

24 These telomeric elements represent a unique case of TE domestication. They serve a critical role for
25 their host genome, yet they are still active elements, capable of causing mutational damage if their
26 activity is left unchecked (Khurana, Xu, Weng, & Theurkauf, 2010; Savitsky, Kravchuk, Melnikova, &
27 Georgiev, 2002; Savitsky, Kwon, Georgiev, Kalmykova, & Gvozdev, 2006). All three elements have
28 been shown to produce abundant piRNAs, and RNAi knockdown of piRNA pathway components leads
29 to their upregulation (Savitsky et al., 2006; Shpiz & Kalmykova, 2011; Shpiz et al., 2011), consistent
30 with the host genome acting to constrain their activity and raising the possibility that, despite being
31 domesticated, these elements are still in conflict with their host (Y. C. Lee, Leek, & Levine, 2017).

32 There are multiple lines of evidence that this is indeed the case: the protein components of *Drosophila*
33 telomeres are rapidly evolving under positive selection, potentially due to a role in preventing the HTT
34 elements from overproliferation (Y. C. Lee et al., 2017). There is a high rate of gain and loss of HTT
35 lineages within the *melanogaster* species group (Saint-Leandre, Nguyen, & Levine, 2019), and there is
36 dramatic variation in telomere length among strains from the *Drosophila* Genetic Reference Panel
37 (DGRP) (Wei et al., 2017). These observations are more consistent with evolution under conflict rather
38 than a stable symbiosis (Saint-Leandre et al., 2019). Furthermore, the nucleotide sequence of the HTT
39 elements evolves extremely rapidly, especially in their unusually long 3' UTRs (Casacuberta & Pardue,
40 2002; Danilevskaya, Tan, Wong, Alibhai, & Pardue, 1998). Within *D. melanogaster*, three *TART*
41 subfamilies have been identified which contain completely different 3' UTRs, and which are known as
42 *TART-A*, *TART-B*, and *TART-C* (Sheen & Levis, 1994).

43 In this study we have characterized the presence of sequence within the coding region of the *D.*
44 *melanogaster nxf2* gene that was previously annotated as an insertion of the *TART-A* transposon
45 (Sackton et al., 2009). We find that the shared homology between *TART-A* and *nxf2* is actually the
46 result of *TART-A* acquiring a portion of the *nxf2* gene, rather than the *nxf2* gene gaining a *TART-A*
47 insertion. We also find that *nxf2* plays a role in suppressing *TART-A* activity, likely via the piRNA
48 pathway. Our findings support a model where *TART-A* produces antisense piRNAs that target *nxf2* for
49 suppression as a counter-defense strategy in response to host silencing. We identified *nxf2* cleavage
50 products from degradome-seq data that are consistent with Aub-directed cleavage of *nxf2* transcripts
51 and we find that, across the *Drosophila* Genetic Reference Panel (DGRP), *TART-A* copy number is
52 negatively correlated with *nxf2* expression. Our findings suggest that TEs can selfishly manipulate host
53 silencing pathways in order to increase their own copy number and that a single TE family can benefit,
54 as well as antagonize, its host genome.

Results

The *TART*-like region of *nxf2* is conserved across the melanogaster group

It was previously reported that the homology between *nxf2* and *TART-A* is due to an insertion of the *TART-A* transposable element in the *nxf2* gene that became fixed in the ancestor of *D. melanogaster* and *D. simulans* (Sackton et al., 2009). To investigate the homology between these elements in more detail, we first extracted 700 bp of sequence from the 3' region of the *nxf2* gene that was annotated as a *TART-A* insertion (**Figure 1A**) and used BLAST (Altschul, Gish, Miller, Myers, & Lipman, 1990) to search this sequence against the *TART-A* RepBase sequence, which was derived from a full-length *TART-A* element cloned from the *iso1 D. melanogaster* reference strain (Abad et al., 2004a). Within the 700 bp segment of *nxf2*, there are four regions of homology between it and the 3' UTR of the *TART-A* consensus sequence. These regions are between 63 bp and 228 bp in length and 93% - 96% sequence identity (**Figure 1B**). The 5' UTR of *TART-A* is copied from its 3' UTR during reverse transcription, which means that, for a given element, both UTRs are identical in sequence (George, Traverse, DeBaryshe, Kelley, & Pardue, 2010). The homology with the *nxf2* 3' UTR is therefore mirrored in the 5' UTR as well (**Figure 1B**).

To investigate the evolutionary origin of the homology between *nxf2* and *TART-A*, we identified *nxf2* orthologs in *D. simulans*, *D. yakuba*, *D. erecta*, *D. biarmipes*, and *D. elegans*. We created a multiple sequence alignment and extracted the sub-alignment corresponding to the 700 bp segment with homology to *TART-A* (**Figure 1C**). The *TART*-like region of *nxf2* is clearly present in all six of these species, which means that, if this portion of the *nxf2* gene was derived from an insertion of a *TART-A* element, the most recent timepoint at which the insertion could have occurred is in the common ancestor of the melanogaster group, ~15 million years ago (Obbard et al., 2012). At the nucleotide level, there is only weak homology between *nxf2* coding sequence and transcripts from more distantly related *Drosophila* species, such as *D. pseudoobscura*. However, at the peptide level, the C-terminal region of Nxf2, which was thought to be derived from *TART-A*, is actually conserved across *Drosophila*, from *D. melanogaster* to *D. virilis* (**Figure S1**), suggesting that, if a *TART-A* element did insert into the *nxf2* gene, it was not a recent event.

A portion of *nxf2* was captured by the *D. melanogaster TART-A* element

If an ancestral *TART-A* element was inserted into the *nxf2* gene in the common ancestor of the melanogaster group, the shared homology between *nxf2* and *TART-A* should be present in most, if not all, extant species in the group. To test this prediction, we obtained the sequences for previously identified *TART-A* homologs from *D. yakuba* and *D. sechellia* (Casacuberta & Pardue, 2002; Villasante et al., 2007). We aligned these sequences to the *D. melanogaster TART-A* consensus sequence and found that the *TART-A* region that shares homology with the *nxf2* gene is only present in the *D. melanogaster TART-A* sequence (**Figure 2A & S2**). Next, we used BLAST to search the canonical *TART-A* sequence against the *D. melanogaster* reference genome. We identified 5 full-length *TART-A* sequences in the assembly (3 from the X chromosome and 2 from the dot chromosome), all of which contain the *nxf2*-like sequence. The *nxf2*-like sequence from these five elements is 100% identical to that from the canonical *TART-A* sequence. We also identified an additional four *TART-A* fragments that overlapped with the *nxf2*-like region. One of the four is also 100% identical to the canonical sequence while the remaining three are between 96%-99% identical to the canonical sequence.

We added these nine sequences to the multiple sequence alignment in **Figure 1C** and inferred a maximum likelihood phylogeny in order to better understand the evolutionary history of the *nxf2/TART* shared homology (**Figure 2B**). The youngest node in the phylogeny represents the split between the *D. melanogaster nxf2* and *TART-A* elements, suggesting that the event leading to the shared homology between these sequences occurred relatively recently, which is consistent with the high degree of sequence similarity between the *D. melanogaster TART-A* and *nxf2* subsequences. Based on these results, we conclude that the *nxf2/TART-A* shared homology is much more likely to have arisen via the recent acquisition of *nxf2* sequence by *TART-A* after the split of *D. melanogaster* from *D. simulans/sechellia*, rather than an insertion of *TART-A* into the *nxf2* gene. The mechanism by which *TART-A* could have acquired a portion of *nxf2* is not clear, however one possibility is via transduction, a

1 process where genomic regions flanking a TE insertion can be incorporated into the TE itself due to
2 aberrant retrotransposition (Moran, DeBerardinis, & Kazazian, 1999; Pickeral, Makalowski, Boguski, &
3 Boeke, 2000).

5 **The *nxf2* gene plays a role in suppressing the activity of *D. melanogaster* telomeric elements**

6 Nxf2 is part of an evolutionarily conserved gene family with functions related to export of RNA from the
7 nucleus (Herold et al., 2000). In *Drosophila*, a paralog of *nxf2* (*nxf1*) has been shown to be involved in
8 the nuclear export of piRNA precursors and the *nxf2* gene itself was identified as a member of the
9 germline piRNA pathway via an RNAi screen (Czech, Preall, McGinn, & Hannon, 2013; Dennis,
10 Brasset, Sarkar, & Vaury, 2016). More recently, several studies have independently shown that Nxf2 is
11 involved in the co-transcriptional silencing of transposons as part of a complex with Nxt1 and
12 Panoramix (Batki et al., 2019; Fabry et al., 2019; Murano et al., 2019; Zhao et al., 2019). To determine
13 whether *nxf2* is involved in the suppression of *TART-A*, we used a short hairpin RNA (shRNA) from the
14 *Drosophila* transgenic RNAi project (TRiP) with a nos-GAL4 driver to target and knockdown expression
15 of *nxf2* in the ovaries. We sequenced total RNA from the *nxf2* knockdown and a control knockdown of
16 the *white* gene. We observed a strong increase in expression for a variety of TE families upon
17 knockdown of *nxf2* (**Figure S3**). The three telomeric elements *HeT-A*, *TAHRE*, and *TART-A*, are
18 among the top 10 most highly upregulated transposable elements, with *HeT-A* showing ~300-fold
19 increase in expression in the *nxf2* knockdown (*TAHRE*: ~110-fold increase, *TART-A*: ~30-fold
20 increase)(**Figure 3**). We repeated the experiment using a shRNA that targeted a different region of *nxf2*
21 and observed a similar pattern and strong correlation between TE expression profiles of both
22 knockdowns (Spearman's rho=0.94, **Figure S4**). These results support previous findings that *nxf2* is a
23 component of the germline piRNA pathway and show that this gene is particularly important for the
24 suppression of the telomeric TEs *HeT-A*, *TAHRE*, and *TART-A*.

26 ***TART-A* piRNAs may target *nxf2* for silencing**

27 Previous studies have reported abundant piRNAs derived from the telomeric TEs, *HeT-A*, *TAHRE* and
28 *TART-A* (Savitsky et al., 2006; Shpiz et al., 2007; Shpiz et al., 2011). We sought to determine whether
29 piRNAs arising from the *nxf2*-like region of *TART-A* could be targeting the *nxf2* gene for downregulation
30 via the piRNA pathway. We used previously published piRNA data from 16 wild-derived strains from the
31 *Drosophila* Genetic Reference Panel (DGRP)(Song et al., 2014). Because the 5' UTR is copied from
32 the 3' UTR, we masked the 5' UTR of *TART-A* before aligning the piRNA data. Among the 16 strains,
33 we found a large variation in *TART-A* piRNA production ranging from 60 – 12,300 reads per million (
34 RPM). From the pool of 16 strains, we identified ~1.3 million reads that aligned to *TART-A*, 98% of
35 which map uniquely (see Methods)(**Figure 4A**). *TART-A* piRNAs have previously been shown to exhibit
36 the 10bp overlap signature of ping-pong cycle amplification (Hur et al., 2016) and we identified both
37 sense and antisense piRNAs arising from *TART-A* (**Figure 4B**) as well as an enrichment of alignments
38 where the 5' end of one piRNA is found directly after the 3' end of the previous piRNA (i.e. 3' to 5'
39 distance of 1), consistent with piRNA phasing (**Figure 4C**). We identified ~95,000 piRNAs arising from
40 the *TART-A* region that shares homology with *nxf2*. Of these reads, 59% are antisense to *TART-A* and
41 41% are sense.

42 We next focused on piRNA production from *nxf2*. We reasoned that, if *nxf2* expression is subject to
43 piRNA-mediated regulation, we should see piRNAs derived from the *nxf2* transcript, outside of the
44 region that shares homology with *TART-A*. We masked the *nxf2/TART-A* region of shared homology
45 and aligned the piRNA sequence data to the *nxf2* transcript. We found low but consistent production of
46 piRNAs from *nxf2* across all 16 DGRP strains (between 1.5 and 41 RPM), with 99.7% of *nxf2*-aligned
47 reads mapping uniquely. To increase sequencing depth, we pooled the data from all 16 strains (2,624
48 *nxf2* reads total) and examined piRNA abundance along the *nxf2* transcript (**Figure 4D**). We found that
49 the most abundant production of piRNAs from *nxf2* occurs at the 3' end of the transcript, downstream
50 from the regions of shared homology with *TART-A* (**Figure 4D**). Overall, 99.4% of reads from *nxf2* are
51 derived from the sense strand of the transcript (**Figure 4E**) and the *nxf2* piRNAs also show evidence of
52 phasing (**Figure 4F**). The enrichment of *nxf2*-derived piRNAs downstream from the region of shared
53 homology with *TART-A*, along with our observation that almost all *nxf2* piRNAs are derived from the

1 sense strand, suggests that these piRNAs are not amplified via the ping-pong cycle, but are instead
2 produced by the Zucchini-mediated phasing process.
3 These results are consistent with a model where antisense piRNAs from the *nxf2*-like region of *TART-A*
4 are bound by Aubergine and targeted to sense transcripts from the *nxf2* gene. Aub cleaves target
5 transcripts between the bases paired to the 10th and 11th nucleotides of its guide piRNA, resulting in a
6 cleavage product with a 5' monophosphate that shares a 10 bp sense:antisense overlap with the guide
7 piRNA that triggered the cleavage. These cleavage products can be enriched and sequenced using an
8 approach known as degradome-seq (Addo-Quaye, Eshoo, Bartel, & Axtell, 2008). We analyzed
9 published degradome-seq and Aub-immunoprecipitated piRNA data from wild-type *D. melanogaster*
10 ovaries (W. Wang et al., 2014) to determine whether we could detect *nxf2* cleavage products resulting
11 from targeting by antisense *TART-A* piRNAs. The degradome-seq data are 100 bp paired-end reads
12 which are long enough to distinguish between the *TART*-like region of *nxf2* and the *nxf2*-like region of
13 *TART-A*. We found three locations within the *TART*-like region of *nxf2* where we observe degradome
14 cleavage products that share the characteristic 10bp sense:antisense overlap with *TART-A* antisense
15 piRNAs (**Figure S5**). These results can be explained under the following model: *TART-A* antisense
16 piRNAs are produced by the ping-pong cycle and bound to Aubergine. A subset of these piRNAs (those
17 from the *nxf2*-like region of *TART-A*) guide Aub to *nxf2* transcripts which are then cleaved. Aub
18 cleavage products can be further processed by Zucchini in the 5' to 3' direction thereby producing
19 phased piRNAs from *nxf2* transcripts downstream from the *nxf2/TART-A* regions of shared homology
20 (**Figure 5**).
21 If piRNAs from *TART-A* are targeting *nxf2* and downregulating its expression, knockdown of piRNA
22 pathway components that either decrease piRNA production from *TART-A* (ping-pong and/or primary
23 piRNA pathway components) or disrupt silencing of *nxf2* (primary piRNA components) should result in
24 an increase in expression of *nxf2*. We analyzed published RNA-seq data from nos-GAL4 driven
25 knockdowns of sixteen genes that were identified as components of the piRNA pathway and that were
26 specifically shown to be involved in repression of *HeT-A* and *TAHRE* (Czech et al., 2013). We
27 compared the expression of *nxf2* in each piRNA component knockdown to its expression in the control
28 knockdown of the *white* gene and found that *nxf2* shows increased expression in 14 of the 16
29 knockdowns, which represents a significant skew towards upregulation (one-sided binomial test
30 $P=0.002$)(**Figure 6**).

31
32 **Natural variation in *TART-A* copy number is correlated with *nxf2* expression levels**
33 Previous work has shown that there is large variation in HTT element copy number at the telomeres of
34 wild *Drosophila* strains (Walter et al., 2007; Wei et al., 2017). Our results predict that, if *TART-A*
35 piRNAs are targeting *nxf2* for suppression, then strains with more copies of *TART-A* should have lower
36 expression of *nxf2*. To test this prediction, we used previously published Illumina genomic sequencing
37 data and microarray gene expression profiles from the *Drosophila* Genetic Reference Panel
38 (DGRP)(Huang et al., 2014; Mackay et al., 2012). We used the Illumina data to infer *TART-A* copy
39 number for 151 DGRP strains (see Methods) and obtained *nxf2* microarray gene expression levels from
40 whole adult females for these same strains. We found that, as predicted, there is a strong negative
41 correlation between *TART-A* copy number and *nxf2* gene expression levels among the DGRP (**Figure**
42 **7**) (Spearman's rho = -0.48, $P=4.6e-10$).

43
44 **Discussion**
45 If the coding sequence of a gene shares sequence homology with a known transposable element, the
46 most likely explanation for this shared homology is that a portion of the gene was derived from a TE
47 insertion. This is, understandably, what was previously reported by Sackton *et al* for the *nxf2* gene and
48 the *TART-A* TE (Sackton et al., 2009), however our analyses are not consistent with such a scenario.
49 Specifically, based on sequence similarity and phylogenetic clustering, the event that created the
50 shared homology between *nxf2* and *TART-A* must have occurred relatively recently, after *D.*
51 *melanogaster* diverged from *D. simulans*, yet the putative insertion of *TART-A* in the *nxf2* gene is
52 shared across *Drosophila*. A scenario that is more consistent with these observations is one where,
53 rather than the *nxf2* gene gaining sequence from *TART-A*, the *TART-A* element captured a portion of
54 the *nxf2* gene, likely via aberrant transcription that extended past the internal *TART-A* poly-A signal to

1 another poly-A signal in the flanking genomic region. This process has been observed for other TEs
2 and is known as exon shuffling or transduction (Moran et al., 1999; Pickeral et al., 2000). Notably, the
3 *nxf2*-like sequence of *TART-A* is located in its 3' UTR, which would be expected if it were acquired via
4 transduction (**Figure 1**). Interestingly, *TART* is part of the LINE family of non-LTR retrotransposons and
5 Human LINE-L1 elements are known to undergo transduction fairly frequently (Goodier, Ostertag, &
6 Kazazian, 2000; Moran et al., 1999; Pickeral et al., 2000). However, transduction would require that an
7 active *TART-A* element was inserted somewhere upstream of the 3' region of *nxf2* at some point in the
8 *D. melanogaster* lineage, but has since been lost from the population. Is this possible given that *TART-A*
9 *A* should only replicate to chromosome ends? The TIDAL-fly database of polymorphic TEs in *D.*
10 *melanogaster* reports several polymorphic *TART-A* insertions far from the chromosome ends, which
11 suggests that this element is occasionally capable of inserting into locations outside of the telomeres
12 (Rahman et al., 2015).

13 The aberrant *TART-A* copy that acquired a portion of the *nxf2* gene most likely arose as a single
14 polymorphic insertion in an ancestral *D. melanogaster* population, yet the *nxf2*-like region of *TART-A* is
15 now present in all full-length *TART-A* elements in the *D. melanogaster* reference genome assembly.
16 We were unable to find any *D. melanogaster* *TART-A* elements in the reference genome, or in
17 GenBank, whose 3' UTR lacks the *nxf2*-like sequence. This suggests that the initially aberrant *TART-A*
18 copy, which acquired a portion of *nxf2*, has now replaced the ancestral *TART-A* element, consistent
19 with the gene acquisition event conferring a fitness benefit to *TART-A*.
20 How could the gene acquisition benefit *TART-A*? We found that the *nxf2*-like region of *TART-A*
21 produces abundant antisense piRNAs that share homology with the *nxf2* gene, and the *nxf2* gene
22 produces additional phased piRNAs from the unique sequence directly downstream from the regions of
23 shared homology (**Figure 4**). These two observations are consistent with a scenario where *TART-*
24 *derived piRNAs* guide Aub proteins to the *nxf2* transcript. The *TART-A* piRNAs may then act as
25 “trigger” piRNAs that catalyze cleavage of *nxf2* transcripts while also resulting in the production of
26 phased piRNAs starting in the region of shared homology and proceeding in the 3' direction to the end
27 of the *nxf2* transcript (**Figure 5**). The piRNA-mediated cleavage of *nxf2* transcripts, which is supported
28 by degradome-seq data (see **Figure S5**), should result in a reduction in *nxf2* expression levels. PiRNA-
29 mediated suppression of *nxf2* is consistent with our finding that disruption of the piRNA pathway by
30 RNAi tends to result in increased *nxf2* expression (**Figure 6**). Given that *nxf2* plays a role in
31 suppressing *TART-A* activity, reduced *nxf2* levels should relieve *TART-A* suppression, which would
32 presumably increase *TART-A* fitness by allowing it to make more copies of itself. Indeed, in the DGRP,
33 we find that individuals with lower *nxf2* expression levels tend to have higher numbers of *TART-A*
34 copies and *vice versa* (**Figure 7**).

35 If additional copies of *TART-A* act to further suppress *nxf2* expression, which then further de-represses
36 *TART-A*, why is there not run-away accumulation of telomere length in *D. melanogaster*? Previous work
37 has shown that long telomeres in *D. melanogaster* are associated with both reduced fertility and
38 fecundity (Walter et al., 2007), so it is possible that a run-away trend towards increasing telomere
39 length is balanced by a fitness cost.

40 Targeting of host transcripts by transposon-derived piRNAs has been previously observed in
41 *Drosophila*. Most notably, piRNAs from the LTR retrotransposons *roo* and *412* play a critical role in
42 embryonic development by targeting complementary sequence in the 3' UTR of the gene *nos*, leading
43 to its repression in the soma (Rouget et al., 2010). More recent results suggest hundreds of maternal
44 transcripts could be regulated in a similar fashion (Barckmann et al., 2015). However, these represent
45 cases where TE piRNAs have been co-opted to regulate host transcripts, whereas our results suggest
46 that the piRNA targeting of *nxf2* is a counter-defense strategy by *TART-A*. This type of strategy has
47 only been previously observed in plants (Cosby et al., 2019). In rice, a CACTA DNA transposon
48 produces a micro-RNA that targets a host methyltransferase gene known to be involved in TE
49 suppression (Nosaka et al., 2012), while in Arabidopsis, siRNAs from *Athila6* retrotransposons target
50 the stress granule protein UBP1b, which is involved in suppressing *Athila6* GAG protein production
51 (McCue et al., 2013).

52 Given that viruses and other pathogens have evolved a variety of methods to block or disrupt host
53 defense mechanisms, it is surprising that there is much less evidence for TEs adopting similar
54 strategies (Cosby et al., 2019). However, unlike viruses, TEs depend heavily on vertical transmission

1 from parent to offspring. Any counter-defense strategy that impacts host fitness would therefore
2 decrease the fitness of the TE as well. Furthermore, disruption of host silencing is likely to lead to
3 upregulation of other TEs, making it more likely that will be a severe decrease in host fitness, similar to
4 what is observed in hybrid dysgenesis. These explanations are relevant to our results: *TART-A* may be
5 targeting *nxf2* for its own advantage, but our knockdown experiment shows that *nxf2* suppression
6 causes upregulation of many other TEs besides *TART-A* (**Figures 3 and S3**) and other studies have
7 shown that *nxf2* mutants are sterile (Batki et al., 2019; Fabry et al., 2019). Why then, does *TART-A*
8 appear to be targeting *nxf2* in spite of these potentially deleterious consequences? One possibility is
9 that the suppression of *nxf2* expression caused by *TART-A* is relatively mild (i.e. much less than the
10 level of down-regulation caused by the RNAi knockdown), which is enough to provide a slight benefit to
11 *TART-A* without causing widespread TE activation. It is also possible that the suppression effect was
12 initially much larger, but has since been counterbalanced by cis-acting variants that increase *nxf2*
13 expression. Future work examining TE activation under varying levels of *nxf2* expression may help to
14 determine whether there is a tipping point where *nxf2* suppression becomes catastrophic.
15 In summary, our results show that so-called domesticated TEs, if active, can still be in conflict with their
16 host and raise the possibility that TE counter-defense strategies may be more common than previously
17 recognized, despite the potentially deleterious consequences for the host.

18 **Methods**

19 ***TART-A* sequence analysis:** We used the *TART-A* sequence from RepBase (Jurka, 2000), which is
20 derived from the sequence reported in (Abad et al., 2004a) (Genbank accession AJ566116). This
21 sequence represents a single full-length *TART-A* element cloned from the *D. melanogaster* iso1
22 reference strain. The *nxf2*-like portion of this sequence is 100% identical to another *TART-A* element
23 cloned and sequenced from *D. melanogaster* strain A4-4 (Genbank DMU02279)(Levis et al., 1993) as
24 well as the *TART-A* sequence from the FlyBase canonical set of transposon sequences (version
25 9.42)(Thurmond et al., 2019) (cloned from *D. melanogaster* strain Oregon-R: Genbank
26 AY561850)(Berlaco, Fanti, Sheen, Levis, & Pimpinelli, 2005).

27 We used BLAST (Altschul et al., 1990) to compare the *TART-A* sequence to the *D. melanogaster nxf2*
28 transcript and visualized BLAST alignments with Kablammo (Wintersinger & Wasmuth, 2015). To
29 compare *TART-A* among *Drosophila* species, we used the *D. yakuba TART-A* sequence reported in
30 (Casacuberta & Pardue, 2002)(GenBank AF468026), which includes the 3' UTR. We also used the *D.*
31 *sechellia TART-A* ORF2 reported by (Villasante et al., 2007)(Genbank AM040251) to search the *D.*
32 *sechellia* FlyBase r1.3 genome assembly for a *TART-A* copy that included the 3' UTR, which we found
33 on scaffold_330:4944-14419. We attempted a similar approach for *D. simulans*, but were unable to find
34 a *TART-A* copy in the *D. simulans* FlyBase r2.02 assembly that included the 3' UTR. We aligned the *D.*
35 *melanogaster*, *D. yakuba* and *D. sechellia TART-A* sequences to each other, and to the *D.*
36 *melanogaster nxf2* transcript (FlyBase FBtr0089479), using nucmer (Kurtz et al., 2004). We then used
37 mummerplot (Kurtz et al., 2004) to create a dotplot to visualize the alignments. To identify all copies of
38 *TART-A* carrying the *nxf2*-like sequence, we used BLAST to search the *TART-A* 3' UTR against the *D.*
39 *melanogaster* release 6 reference genome.

40 ***nxf2* sequence analysis:** We downloaded *nxf2* transcripts from the NCBI RefSeq database for
41 *Drosophila simulans* (XM_016169386.1), *yakuba* (XM_002095083.2), *erecta* (XM_001973010.3),
42 *biarmipes* (XM_017111057.1), and *elegans* (XM_017273027.1) and created a codon-aware multiple
43 sequence alignment using PRANK (Loytynoja, 2014), which we visualized with JalView (Waterhouse,
44 Procter, Martin, Clamp, & Barton, 2009). To compare Nxf2 peptide sequences, we used the web
45 version of NCBI BLAST to search the *D. melanogaster Nxf2* peptide sequence against all *Drosophila*
46 peptide sequences present in the RefSeq database. We then used the NCBI COBALT (Papadopoulos
47 & Agarwala, 2007) multiple-sequence alignment tool to align the sequences shown in **Figure S1**.

48 ***TART-A/nxf2* gene tree:** We extracted the *nxf2*-like sequences from all *TART-A* copies present in the
49 *D. melanogaster* reference genome and aligned them to the *TART*-like *nxf2* sequences from seven
50 *Drosophila* species using PRANK. We then inferred a maximum likelihood phylogeny with 100
51 bootstrap replicates using RAxML (Stamatakis, 2014).

52 ***nxf2* knockdown:** We used two different strains from the *Drosophila* Transgenic RNAi Project (TRiP)
53 that express dsRNA for RNAi of *nxf2* (Bloomington #34957 & #33985), as well as a control strain for
54

1 RNAi of the *white* gene (Bloomington #33613). Seven males of each of these strains were crossed to
2 seven, 3-5 day old, virgin females carrying the nos-GAL4 driver (Bloomington #25751). After 6 days of
3 mating, we discarded the parental flies and then transferred F1 offspring to fresh food for 2.5 days
4 before collecting ovaries from six females for each cross. We performed two biological replicates for
5 each of the three crosses, dissected the ovaries in 1x PBS and immediately transferred them to
6 RNAlater. We extracted RNA using Trizol/Phenol-Chloroform and used the AATI Fragment Analyzer to
7 assess RNA integrity. We then prepared stranded, total RNA-seq libraries by first depleting rRNA with
8 ribo-zero and then using the NEBnext ULTRA II library prep kit to prepare the sequencing libraries. The
9 libraries were sequenced on the Illumina NextSeq machine with 150 bp paired-end reads.

10 ***nxf2* knockdown RNA-seq analysis:** The average insert sizes of the total RNA-seq libraries were less
11 than 300 bp, which resulted in overlapping mate pairs for the majority of sequenced fragments. Instead
12 of analyzing these data as paired-end reads, we instead merged the overlapping mates to generate
13 single-end reads using BBmerge (Bushnell, Rood, & Singer, 2017). We removed rRNA and tRNA
14 contamination from the merged reads by aligning them to all annotated rRNA and tRNA sequences in
15 the *D. melanogaster* reference genome using Hisat2 (Kim, Langmead, & Salzberg, 2015) and retained
16 all unaligned reads. In order to quantify expression from genes as well as TEs, we combined all *D.*
17 *melanogaster* transcript sequences (FlyBase version 6.26) with *D. melanogaster* RepBase TE
18 consensus sequences. We accounted for multi-mapping reads by using bowtie2 (Langmead &
19 Salzberg, 2012) to align each read to all possible alignment locations (using *--all* and *--very-sensitive-*
20 *local*) and then using eXpress (Roberts & Pachter, 2013) to estimate FPKM values, accounting for the
21 multi-mapped alignments. We averaged FPKM values between biological replicates and assessed the
22 reproducibility of both TE and gene expression profiles in the *nxf2* knockdown by comparing the results
23 from the two different dsRNA hairpins.

24 **piRNA analysis:** We analyzed previously published piRNA data from 16 strains from the Drosophila
25 Genetic Reference Panel (DGRP)(Song et al., 2014). We used cutadapt (Martin, 2011) to trim adapter
26 sequences from each library and then removed rRNA and tRNA sequences by using bowtie
27 (Langmead, 2010) to align the reads to all annotated rDNA and tRNA genes in the *D. melanogaster*
28 reference genome, retaining the reads that did not align. We then created a reference database
29 composed of the following sequence sets: a hard-masked version of the *D. melanogaster* reference
30 genome assembly (release 6) where all TE sequences and the *nxf2* gene were replaced by N's using
31 RepeatMasker, the full set of *D. melanogaster* RepBase TE consensus sequences, and the *nxf2*
32 transcript, with its *TART*-like region replaced by N's. We used the unique-weighting mode in ShortStack
33 (Axtell, 2013; Johnson, Yeoh, Coruh, & Axtell, 2016) to align the piRNA reads to this reference
34 database. With this mode, ShortStack probabilistically aligns multi-mapping reads based on the
35 abundance of uniquely mapping reads in the flanking region. We then used the ShortStack alignments
36 and Bedtools (Quinlan & Hall, 2010) to calculate coverage for sense and antisense alignments to
37 *TART-A* as well as *nxf2*. To test for evidence of piRNA phasing, we used the formula described in (Han
38 et al., 2015)

39 **piRNA component knockdowns:** We used the RNA-seq counts for *nxf2* reported in GEO accession
40 GSE117217 from 16 RNAi knockdowns of piRNA pathway components as well as a control knockdown
41 of the *Yb* gene (Czech et al., 2013). For each knockdown, we normalized *nxf2* expression by dividing
42 the raw counts by the sum of all gene counts and reported the result in Reads Per Million (RPM).

43 **Degradome-seq analysis:** We used degradome-seq and Aub-immunoprecipitated small RNA data
44 from wild-type *D. melanogaster* strain w1 (W. Wang et al., 2014). We used bowtie2 to align the
45 degradome-seq data to the same reference sequence used in the piRNA analysis except we unmasked
46 the *nxf2* transcript. We analyzed the small RNA data as described under "piRNA analysis" and then
47 used bedtools to extract degradome read alignments whose 5' end was located in the *TART*-like region
48 of *nxf2* and antisense small RNA alignments whose 5' end was located in the *nxf2*-like region of *TART-*
49 *A* and whose length was consistent with piRNAs (23-30 bp). We then used bowtie to align the minus
50 strand piRNAs to the *nxf2* transcript and used bedtools to identify piRNAs whose 5' end overlapped the
51 5' of degradome reads by 10 basepairs.

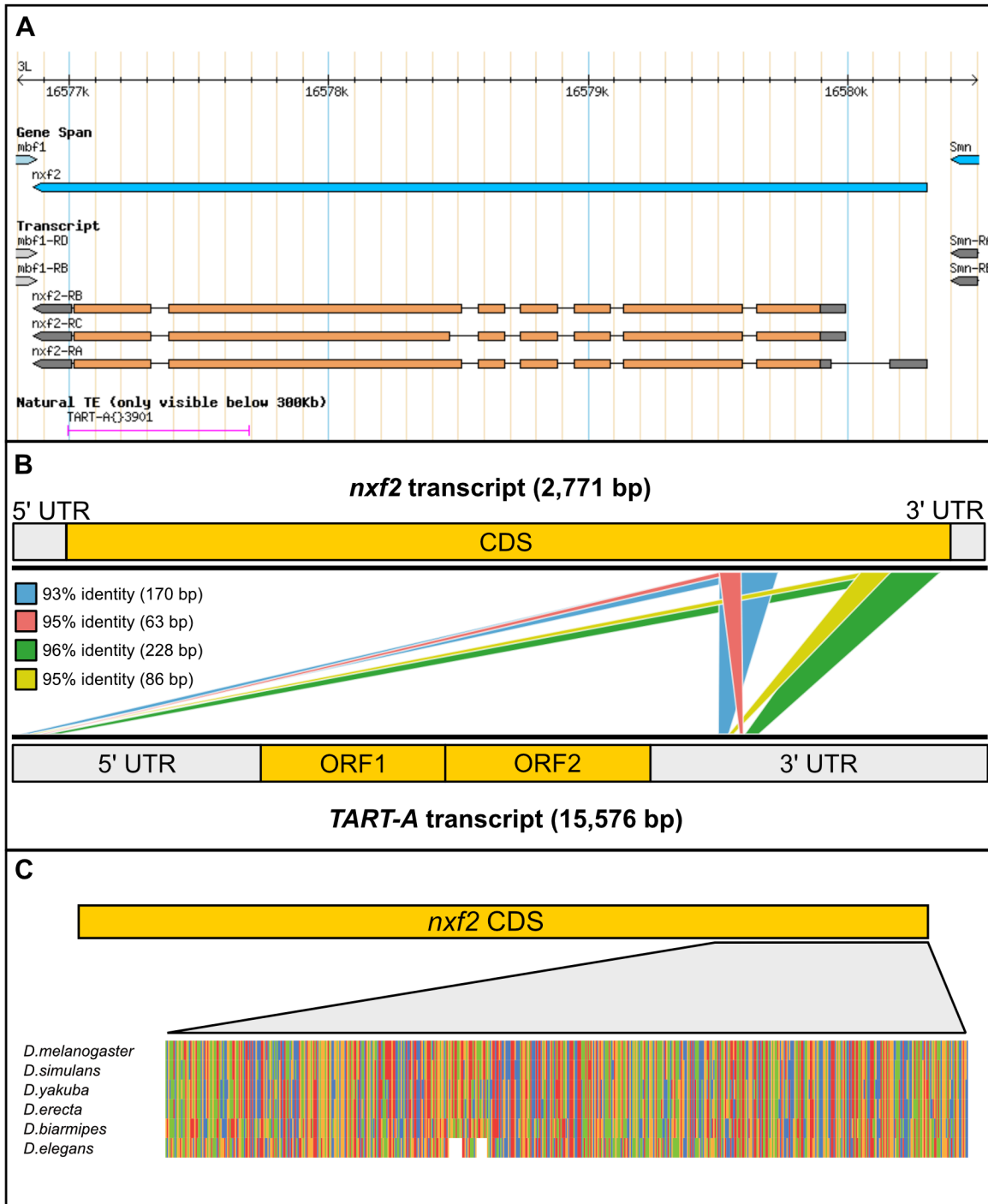
52 ***TART-A* copy number variation and *nxf2* expression:** We used Illumina genomic sequencing data
53 from the DGRP (Huang et al., 2014; Mackay et al., 2012) to estimate *TART-A* copy number. Across
54 strains, the DGRP Illumina data differs in terms of coverage, read length, and paired versus single-end

1 data. To attempt to control for these differences, we trimmed all reads to 75 bp and treated all data as
2 single-end. We also downsampled all libraries to ~13 million reads. We first trimmed each strain's
3 complete dataset (unix command: `zcat file.fastq.gz | cut -c 75`) and then aligned the trimmed reads to
4 the *D. melanogaster* release 6 genome assembly using bowtie2 with the `--very-sensitive` option. We
5 then corrected the resulting bam file for GC bias using DeepTools (Ramirez, Dundar, Diehl, Gruning, &
6 Manke, 2014) and counted the number of aligned reads in the corrected bam file using samtools (Li et
7 al., 2009). We removed all strains with less than 13 million aligned reads and, for each remaining strain,
8 we calculated the fraction of reads to keep by dividing the smallest number of aligned reads across all
9 remaining individuals (13,594,737) by the total number of aligned reads for that strain. We then used
10 this fraction to randomly downsample the GC corrected bam file using the `subsample` option from
11 `samtools view` (Li et al., 2009). We converted each bam file to a fastq file with `samtools fastq` and
12 aligned the fastq file to the *D. melanogaster* RepBase TE sequences with `bowtie2` using the `--very-`
13 `sensitive`, `--local`, and `--all` options. With `--all`, `bowtie2` reports every possible alignment for each multi-
14 mapping sequence. We then used `eXpress` to retain a single alignment for each multi-mapping
15 sequence based on the abundance of neighboring unique alignments. We used the `eXpress` bam files
16 to calculate the median per-base coverage (excluding positions with coverage of zero) for the *TART-A*
17 coding sequence (i.e. ORF1 & ORF2), for each individual. To estimate *TART-A* copy number, we
18 divided the median *TART-A* coverage of each strain by that strain's median per-base coverage of all
19 uniquely-mappable positions in the *D. melanogaster* reference genome (calculated from the GC
20 corrected, downsampled bam file). Uniquely-mappable positions were identified using `mirth`
21 (<https://github.com/EvolBioInf/mirth>). We obtained *nxf2* expression values from previously published
22 microarray gene expression profiles from whole adult females for all DGRP strains (Huang et al., 2015).

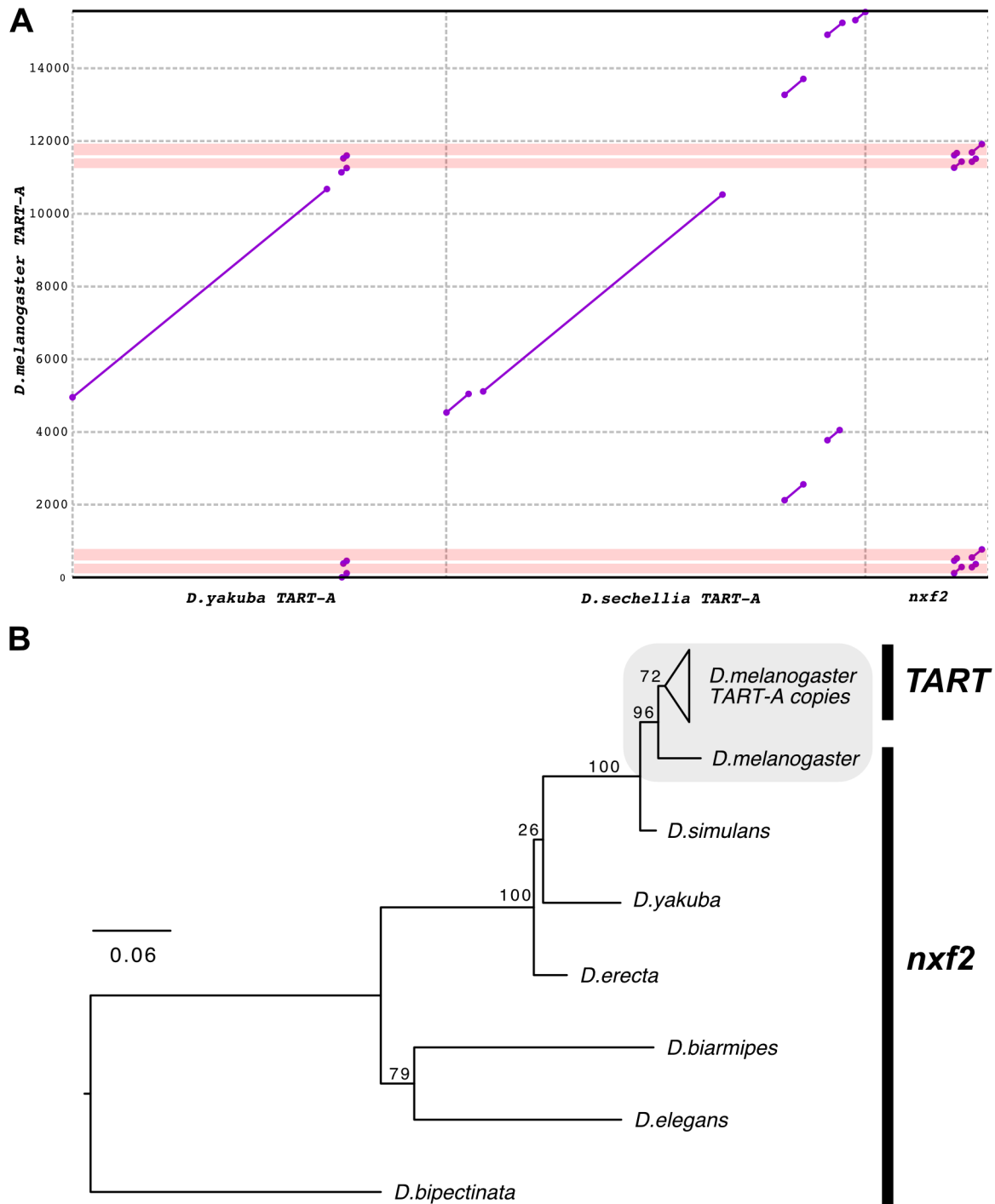
23
24
25
26
27
28
29
30
31
32
33
34
35
36
37
38
39
40
41
42
43
44
45
46
47
48
49
50
51
52
53
54

1 **Figures**

2



3
4 **Figure 1. Shared homology between the *D. melanogaster nxf2* gene and the *TART-A***
5 **transposable element.** (A) GBrowse screenshot from FlyBase showing the *nxf2* gene model along
6 with the annotated *TART-A* TE insertion. Note that the *TART-A* annotation overlaps the 3' coding
7 sequence of *nxf2*. (B) BLAST hits between the RepBase *TART-A* sequence and the *nxf2* transcript.
8 Each colored box represents a single BLAST alignment. The 5' UTR of *TART-A* is copied from its 3'
9 UTR during replication. The two UTRs are therefore identical in sequence and the homology between
10 *nxf2* and the *TART-A* 3' UTR is mirrored in the 5' UTR. (C). A zoomed-out multiple sequence alignment
11 of *nxf2* orthologs for six species from the melanogaster species group shows that the *TART-like* region
12 of *nxf2* is present in all six species.



1 **Figure 2. The TART-A/nxf2 homology is unique to *D. melanogaster*.**
2 (A) Dotplot comparing *D. melanogaster* TART-A to its homologs in *D. yakuba* and *D. sechellia*. The
3 diagonal lines denote regions of homology while the pink boxes show the location of the *nxf2*-like
4 sequence in the *D. melanogaster* TART-A. Neither the *D. yakuba* nor the *D. sechellia* TART-A
5 sequences contain *nxf2*-like sequence. However, the regions directly flanking the *nxf2*-like sequence in
6 *D. melanogaster* are also present in *D. yakuba* (see **Figure S2** for magnified view). (B) Gene tree
7 showing relative age of shared homology. We aligned the *nxf2*-like sequences from nine copies of
8 TART-A in the *D. melanogaster* reference genome to the *nxf2* transcripts from six *Drosophila* species
9 and inferred a maximum likelihood phylogeny using RAxML. *D. melanogaster* *nxf2* is most closely
10 related to the *nxf2*-like sequences present in the *D. melanogaster* TART-A copies, suggesting the
11 shared homology occurred after the divergence between *D. melanogaster* and *D. simulans*.

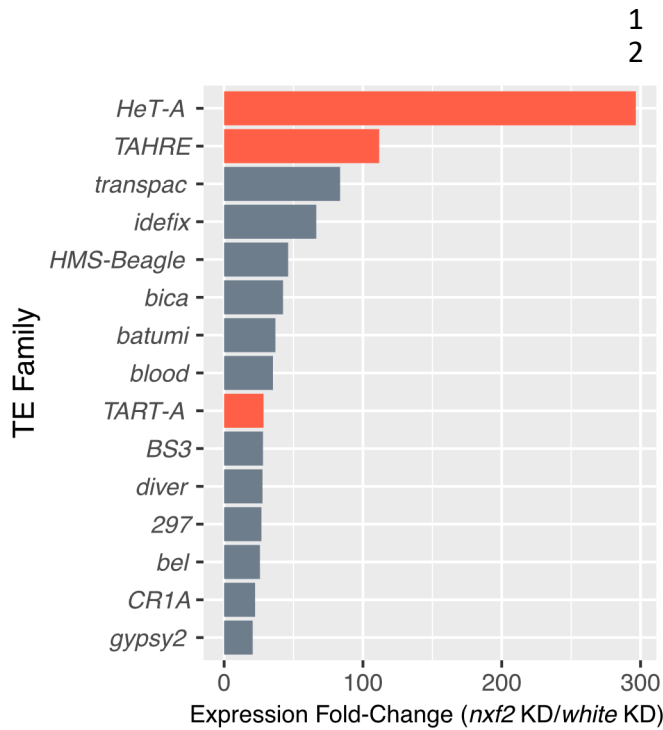


Figure 3. RNAi knockdown of *nxf2* leads to strong upregulation of HTT elements.

We examined TE expression profiles using RNA-seq of total RNA from ovaries in a *nxf2* knockdown versus a control knockdown of the *white* gene. We found that a variety of transposable elements show increased expression in the *nxf2* knockdown (see **Figure S3** for all TEs), however the three telomeric HTT elements (red bars) are among the top 10 most highly upregulated TEs.

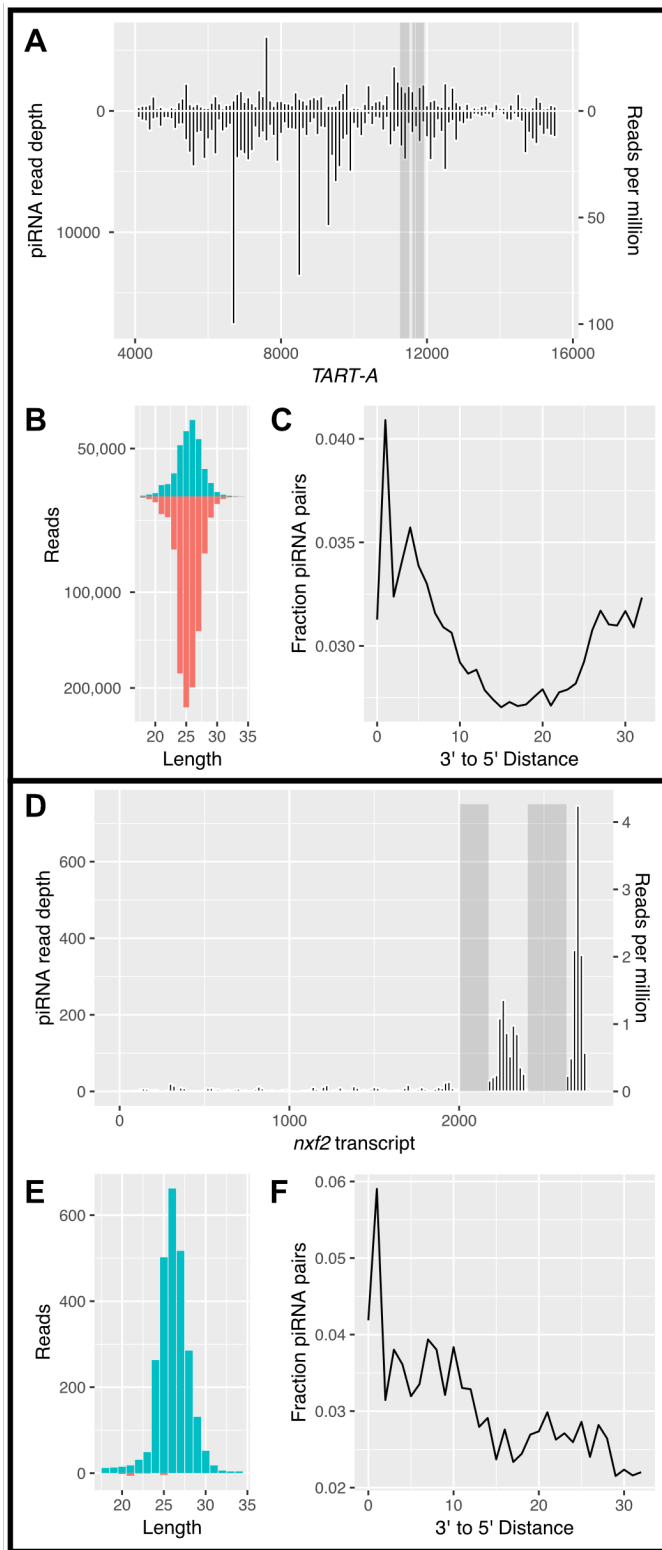


Figure 4. piRNAs are produced from both *TART-A* and *nxf2*

(A) We aligned previously published piRNA data from the *D. melanogaster* Drosophila Genetic Reference Panel (DGRP)(Song et al., 2014) to *TART-A* and examined read coverage across the element. We find abundant sense and antisense piRNA production across most of the element, including the regions containing the *nxf2*-like sequence (grey boxes). Note that the 5' UTR of *TART-A* is copied from the 3' UTR during replication and is therefore identical in sequence. We masked the 5' UTR (positions 1-4000) for this analysis. (B) The length of aligned reads are consistent with that expected for piRNAs and the *TART-A* derived piRNAs are biased towards the minus strand. (C) *TART-A* piRNAs show an enrichment of alignments where the 5' end of one piRNA is found directly after the 3' end of the previous piRNA (i.e. distance of 1), consistent with piRNA phasing. (D) Unlike *TART-A*, *nxf2* produces piRNAs primarily in the regions directly downstream from its *TART*-like sequence (grey boxes). The vast majority of these piRNAs are only from the sense strand of *nxf2* (panel E) and also show the signature of phasing (panel F). Note that the *TART*-like sequence of *nxf2* was masked for this analysis to avoid cross-mapping of *TART*-derived piRNAs to the *nxf2* transcript.

TART-A produces antisense piRNAs via ping-pong cycle

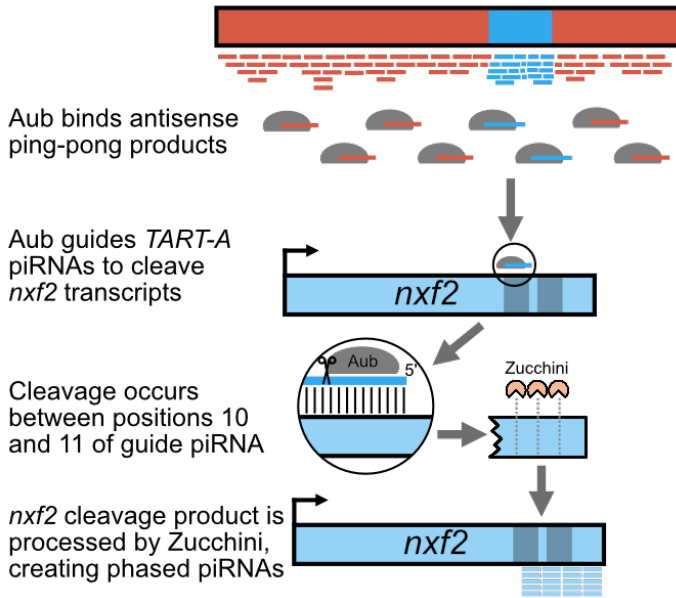


Figure 5. Model describing generation of phased piRNAs from *nxf2*

TART-A produces abundant antisense piRNAs derived from ping-pong amplification, including from the TART-A/*nxf2* region of shared homology (blue box on red background). The PIWI protein Aubergine binds antisense ping-pong piRNAs, a subset of which share homology with *nxf2*. These piRNAs guide Aub to *nxf2* and result in cleavage of the transcript between the 10th and 11th nucleotide of the guide piRNA. Transcript cleavage creates an *nxf2* cleavage product that shares a 10 bp sense:antisense overlap with the guide piRNA (see **Figure S5**). The *nxf2* cleavage product can be subsequently processed by the Zucchini endonuclease, creating phased piRNAs starting from the site of Aub cleavage and proceeding to the 3' end of the *nxf2* transcript.

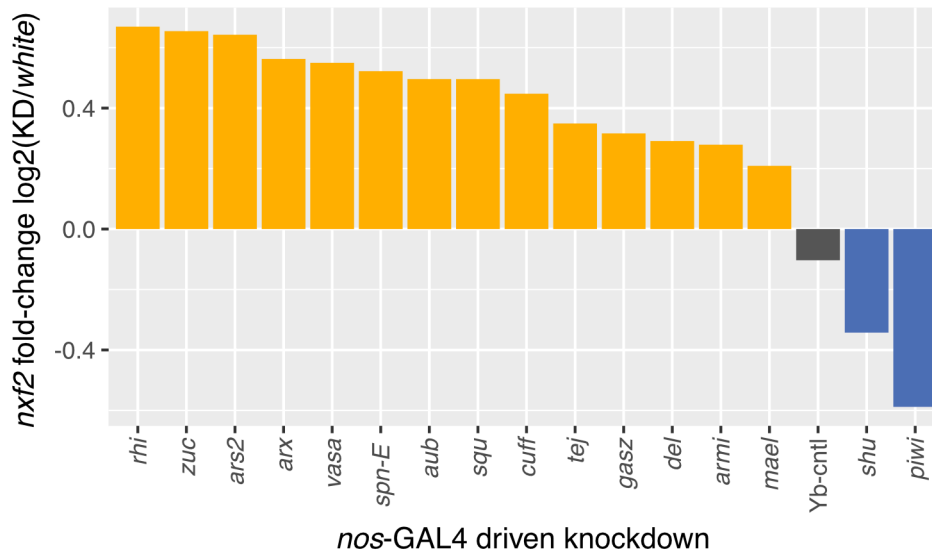


Figure 6. Knockdown of piRNA pathway components is associated with upregulation of *nxf2*.

If TART-derived piRNAs are targeting *nxf2* for suppression, disruption of the piRNA pathway should relieve this suppression. We examined previously published RNA-seq data from 16 piRNA component knockdowns, as well as a control (*Yb*)(Czech et al., 2013). *Nxf2* expression increased in 14 out of 16 knockdowns, significantly more than expected by chance (one-sided binomial test $P=0.002$).

1

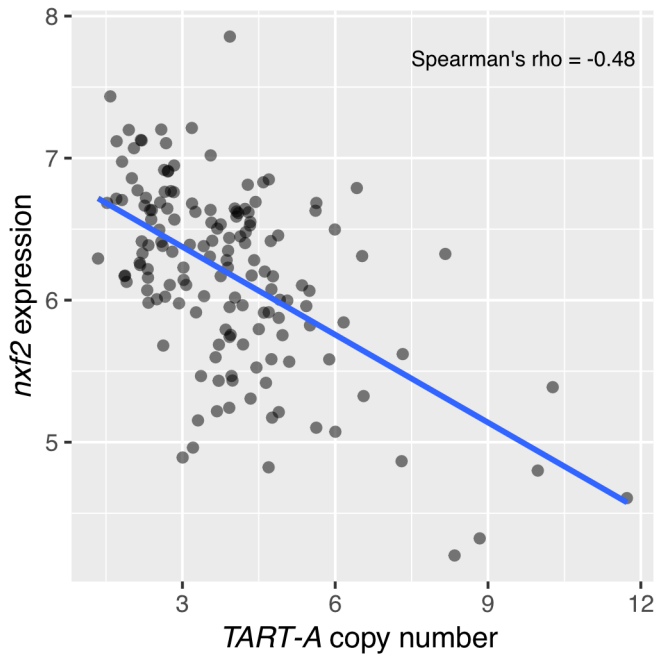
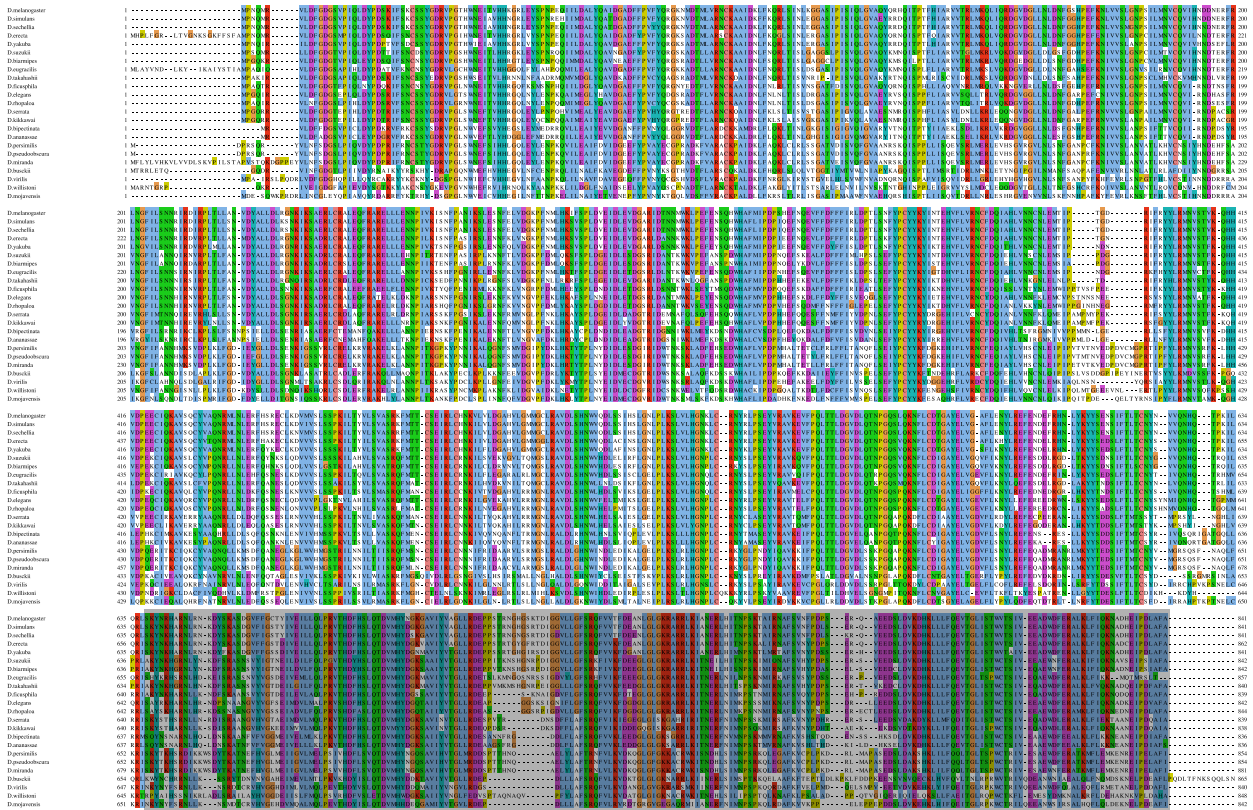


Figure 7. *TART-A* copy number is negatively correlated with *nxf2* expression across the *Drosophila* Genetic Reference Panel (DGRP). We inferred *TART-A* copy-number for 151 DGRP strains using published Illumina sequencing data (Huang et al., 2014; Mackay et al., 2012) and retrieved expression values for *nxf2* from microarray data from whole adult females (Huang et al., 2015). We found that *TART-A* copy number is significantly negatively correlated with *nxf2* expression levels, as expected if *TART-A* piRNAs are targeting *nxf2* for suppression (Spearman's rho = -0.48, P = 4.6e-10).

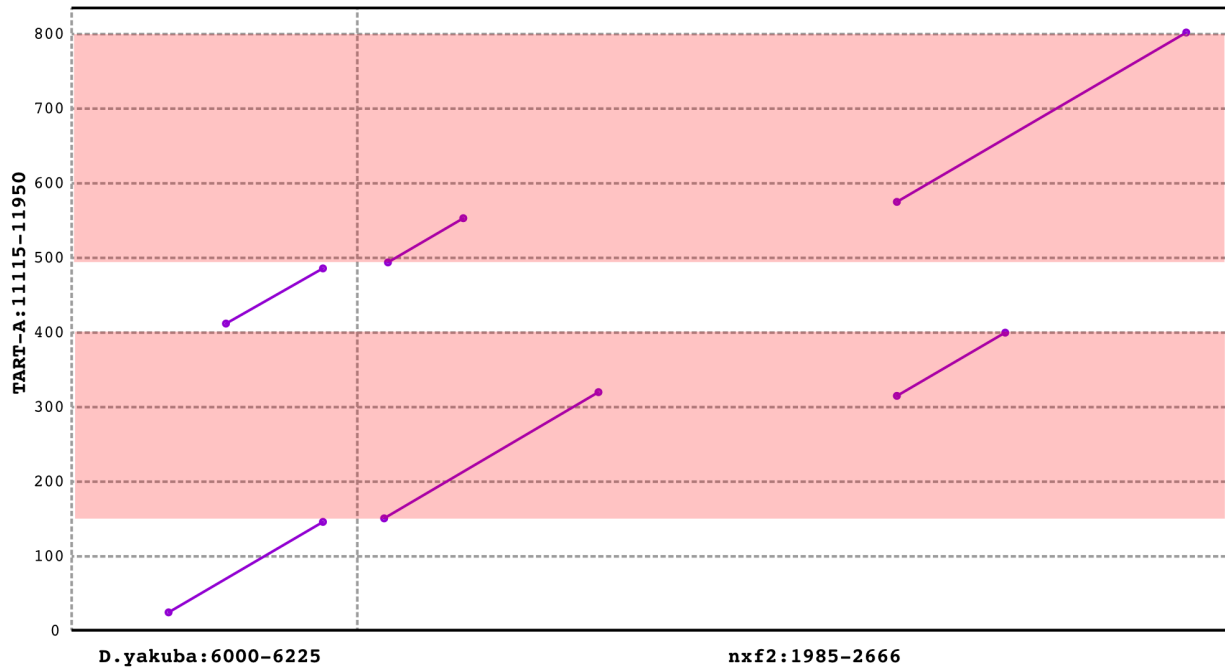
22
23

24
25
26
27
28
29
30
31
32
33
34
35
36
37
38
39
40
41
42
43
44
45
46
47
48
49
50
51
52
53
54

1 Supplemental Figures



- 2 **Figure S1 Peptide alignment of Nxf2 homologs.** We used NCBI web BLAST to search the *D.*
3 *melanogaster* Nxf2 peptide sequence against the RefSeq peptide database and identified homologs in
4 22 Drosophila species. The C-terminal region of Nxf2 derives from coding sequence which shares
5 homology with the *TART-A* transposable element (grey box). At the peptide level, this region is
6 conserved out to *D. virilis*, which suggests that, if it was acquired from an insertion of the *TART-A* TE,
7 the insertion would have occurred in the common ancestor of the entire genus.
8



- 1 **Figure S2. Zoom view of dotplot showing alignments of *D. melanogaster* TART-A versus *D.***
- 2 ***melanogaster* nxf2 and *D. yakuba* TART-A.** The pink boxes show the two segments of shared
- 3 homology between *D. melanogaster* TART-A and *D. melanogaster* nxf2. *D. yakuba* TART-A aligns to
- 4 *D. melanogaster* TART-A at regions directly adjacent to, but not including, the TART-A/nxf2 shared
- 5 homology.
- 6

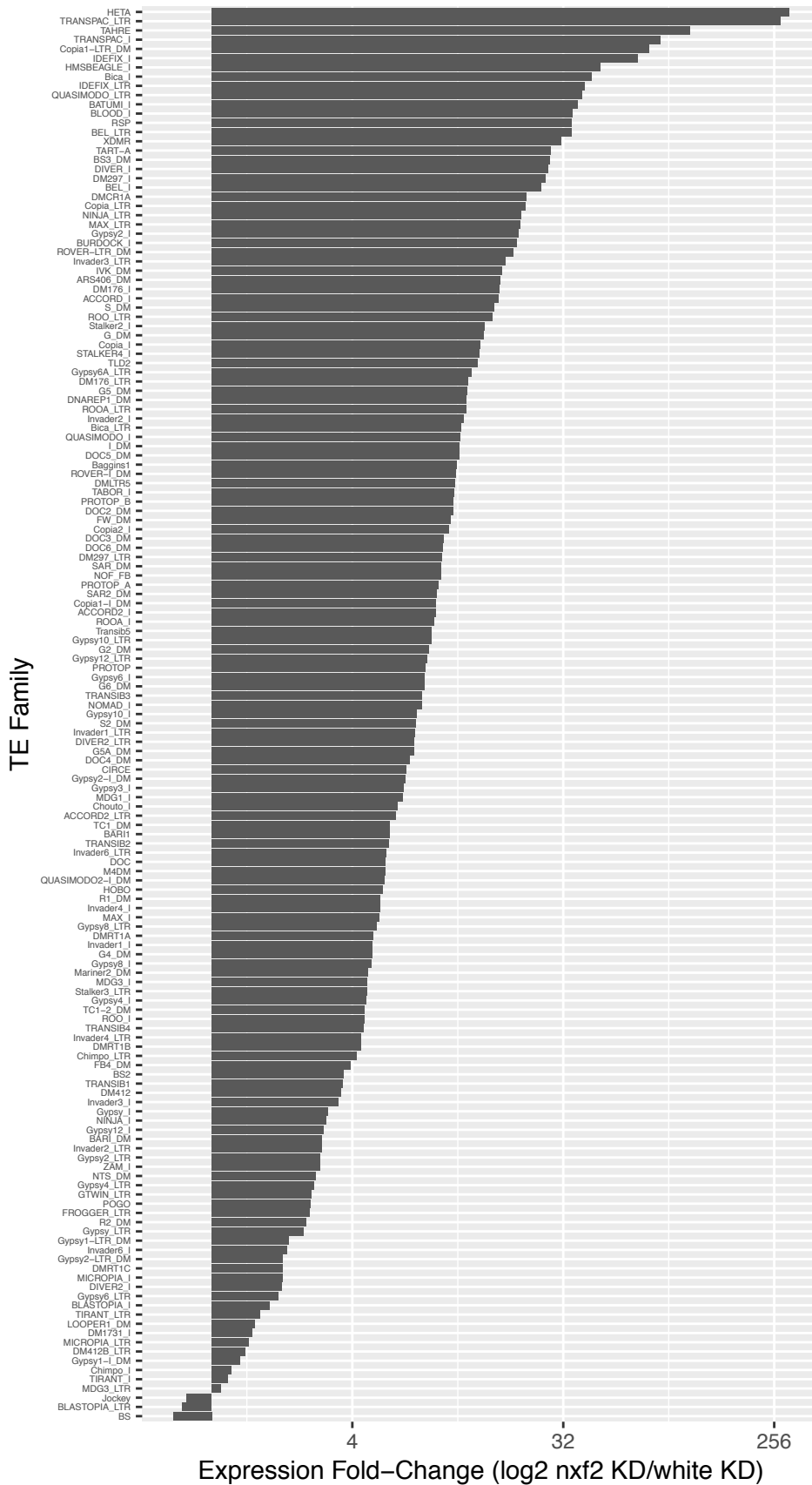
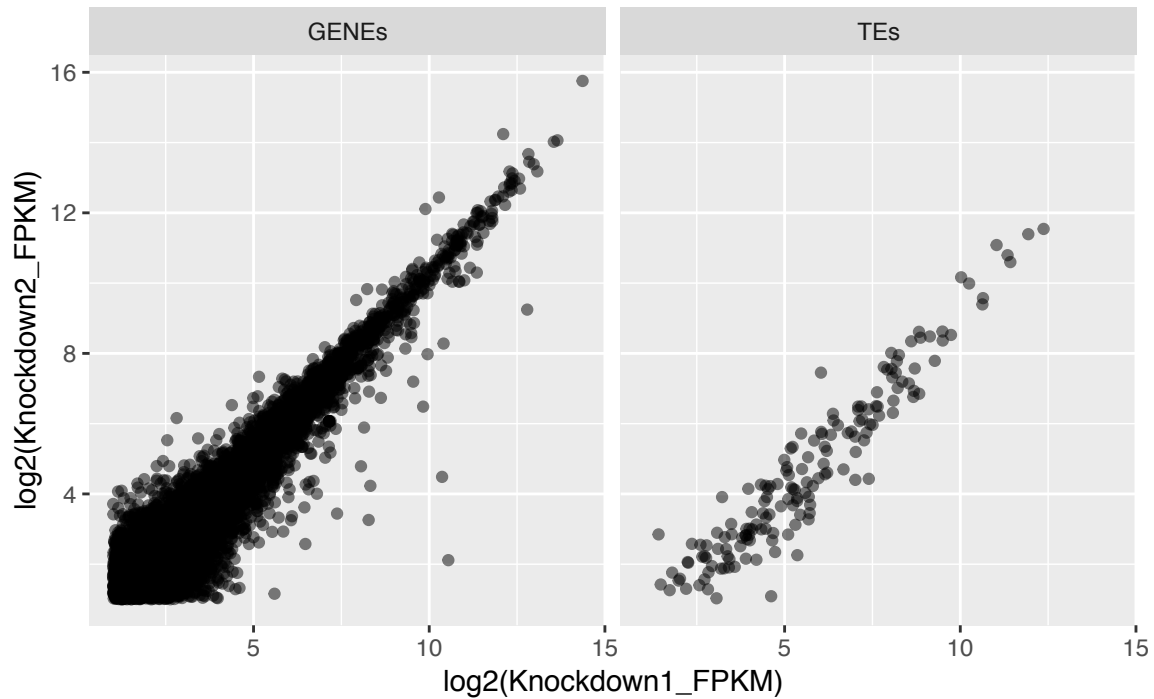


Figure S3 Repetitive element upregulation in *nxf2* knockdown. Each RepBase repeat for which we observed expression in total RNA-seq data from female ovaries is shown on the y-axis and the fold-change in expression in the *nxf2* RNAi knockdown versus a control knockdown of the *white* gene is shown on the x-axis with a log₂ scale. Expression values are the mean of two biological replicates for both knockdown and control. For LTR retrotransposons, LTRs are shown separately from the rest of the TE.



1 **Figure S4 Correlation between shRNAs in *nxf2* knockdown.**
2 We used two shRNAs that target different regions of the *nxf2* transcript and calculated expression
3 values for genes as well as TEs for each knockdown. We found that the expression values are highly
4 correlated between the two experiments (Spearman's rho=0.92 [Genes] and 0.94 [TEs]).
5
6
7
8
9

10
11
12
13
14
15
16
17
18
19
20
21
22
23
24
25
26
27
28
29
30
31

References

- 1
2
- 3 Abad, J. P., De Pablos, B., Osoegawa, K., De Jong, P. J., Martin-Gallardo, A., & Villasante, A. (2004a).
4 Genomic analysis of *Drosophila melanogaster* telomeres: full-length copies of HeT-A and TART
5 elements at telomeres. *Mol Biol Evol*, *21*(9), 1613-1619. doi:10.1093/molbev/msh174
- 6 Abad, J. P., De Pablos, B., Osoegawa, K., De Jong, P. J., Martin-Gallardo, A., & Villasante, A. (2004b).
7 TAHRE, a novel telomeric retrotransposon from *Drosophila melanogaster*, reveals the origin of
8 *Drosophila* telomeres. *Mol Biol Evol*, *21*(9), 1620-1624. doi:10.1093/molbev/msh180
- 9 Addo-Quaye, C., Eshoo, T. W., Bartel, D. P., & Axtell, M. J. (2008). Endogenous siRNA and miRNA
10 targets identified by sequencing of the *Arabidopsis* degradome. *Curr Biol*, *18*(10), 758-762.
11 doi:10.1016/j.cub.2008.04.042
- 12 Altschul, S. F., Gish, W., Miller, W., Myers, E. W., & Lipman, D. J. (1990). Basic local alignment search
13 tool. *J Mol Biol*, *215*(3), 403-410. doi:10.1016/S0022-2836(05)80360-2
- 14 Axtell, M. J. (2013). ShortStack: comprehensive annotation and quantification of small RNA genes. *RNA*,
15 *19*(6), 740-751. doi:10.1261/rna.035279.112
- 16 Barckmann, B., Pierson, S., Dufourt, J., Papin, C., Armenise, C., Port, F., . . . Simonelig, M. (2015).
17 Aubergine iCLIP Reveals piRNA-Dependent Decay of mRNAs Involved in Germ Cell Development
18 in the Early Embryo. *Cell Rep*, *12*(7), 1205-1216. doi:10.1016/j.celrep.2015.07.030
- 19 Batki, J., Schnabl, J., Wang, J., Handler, D., Andreev, V. I., Stieger, C. E., . . . Brennecke, J. (2019). The
20 nascent RNA binding complex SFINX licenses piRNA-guided heterochromatin formation. *Nat*
21 *Struct Mol Biol*, *26*(8), 720-731. doi:10.1038/s41594-019-0270-6
- 22 Berloco, M., Fanti, L., Sheen, F., Levis, R. W., & Pimpinelli, S. (2005). Heterochromatic distribution of
23 HeT-A- and TART-like sequences in several *Drosophila* species. *Cytogenet Genome Res*, *110*(1-
24 4), 124-133. doi:10.1159/000084944
- 25 Biessmann, H., & Mason, J. M. (1997). Telomere maintenance without telomerase. *Chromosoma*,
26 *106*(2), 63-69.
- 27 Biessmann, H., Valgeirsdottir, K., Lofsky, A., Chin, C., Ginther, B., Levis, R. W., & Pardue, M. L. (1992).
28 HeT-A, a transposable element specifically involved in "healing" broken chromosome ends in
29 *Drosophila melanogaster*. *Mol Cell Biol*, *12*(9), 3910-3918. doi:10.1128/mcb.12.9.3910
- 30 Blumenstiel, J. P., Erwin, A. A., & Hemmer, L. W. (2016). What Drives Positive Selection in the
31 *Drosophila* piRNA Machinery? The Genomic Autoimmunity Hypothesis. *Yale J Biol Med*, *89*(4),
32 499-512.
- 33 Bohne, A., Brunet, F., Galiana-Arnoux, D., Schultheis, C., & Volff, J. N. (2008). Transposable elements as
34 drivers of genomic and biological diversity in vertebrates. *Chromosome Res*, *16*(1), 203-215.
35 doi:10.1007/s10577-007-1202-6
- 36 Brennecke, J., Aravin, A. A., Stark, A., Dus, M., Kellis, M., Sachidanandam, R., & Hannon, G. J. (2007).
37 Discrete small RNA-generating loci as master regulators of transposon activity in *Drosophila*.
38 *Cell*, *128*(6), 1089-1103. doi:10.1016/j.cell.2007.01.043
- 39 Bushnell, B., Rood, J., & Singer, E. (2017). BBMerge - Accurate paired shotgun read merging via overlap.
40 *PLoS One*, *12*(10), e0185056. doi:10.1371/journal.pone.0185056
- 41 Cam, H. P., Noma, K., Ebina, H., Levin, H. L., & Grewal, S. I. (2008). Host genome surveillance for
42 retrotransposons by transposon-derived proteins. *Nature*, *451*(7177), 431-436.
43 doi:10.1038/nature06499
- 44 Casacuberta, E., & Pardue, M. L. (2002). Coevolution of the telomeric retrotransposons across
45 *Drosophila* species. *Genetics*, *161*(3), 1113-1124.

- 1 Chang, C. H., Chavan, A., Palladino, J., Wei, X., Martins, N. M. C., Santinello, B., . . . Mellone, B. G.
2 (2019). Islands of retroelements are major components of *Drosophila* centromeres. *PLoS Biol*,
3 17(5), e3000241. doi:10.1371/journal.pbio.3000241
- 4 Chueh, A. C., Northrop, E. L., Brettingham-Moore, K. H., Choo, K. H., & Wong, L. H. (2009). LINE
5 retrotransposon RNA is an essential structural and functional epigenetic component of a core
6 neocentromeric chromatin. *PLoS Genet*, 5(1), e1000354. doi:10.1371/journal.pgen.1000354
- 7 Chuong, E. B., Elde, N. C., & Feschotte, C. (2016). Regulatory evolution of innate immunity through co-
8 option of endogenous retroviruses. *Science*, 351(6277), 1083-1087.
9 doi:10.1126/science.aad5497
- 10 Chuong, E. B., Elde, N. C., & Feschotte, C. (2017). Regulatory activities of transposable elements: from
11 conflicts to benefits. *Nat Rev Genet*, 18(2), 71-86. doi:10.1038/nrg.2016.139
- 12 Chuong, E. B., Rumi, M. A., Soares, M. J., & Baker, J. C. (2013). Endogenous retroviruses function as
13 species-specific enhancer elements in the placenta. *Nat Genet*, 45(3), 325-329.
14 doi:10.1038/ng.2553
- 15 Cosby, R. L., Chang, N. C., & Feschotte, C. (2019). Host-transposon interactions: conflict, cooperation,
16 and cooption. *Genes Dev*, 33(17-18), 1098-1116. doi:10.1101/gad.327312.119
- 17 Crysanto, D., & Obbard, D. J. (2019). Widespread gene duplication and adaptive evolution in the RNA
18 interference pathways of the *Drosophila obscura* group. *BMC Evol Biol*, 19(1), 99.
19 doi:10.1186/s12862-019-1425-0
- 20 Czech, B., Preall, J. B., McGinn, J., & Hannon, G. J. (2013). A transcriptome-wide RNAi screen in the
21 *Drosophila* ovary reveals factors of the germline piRNA pathway. *Mol Cell*, 50(5), 749-761.
22 doi:10.1016/j.molcel.2013.04.007
- 23 Danilevskaya, O. N., Tan, C., Wong, J., Alibhai, M., & Pardue, M. L. (1998). Unusual features of the
24 *Drosophila melanogaster* telomere transposable element HeT-A are conserved in *Drosophila*
25 *yakuba* telomere elements. *Proc Natl Acad Sci U S A*, 95(7), 3770-3775.
26 doi:10.1073/pnas.95.7.3770
- 27 Dennis, C., Brasset, E., Sarkar, A., & Vaury, C. (2016). Export of piRNA precursors by EJC triggers
28 assembly of cytoplasmic Yb-body in *Drosophila*. *Nat Commun*, 7, 13739.
29 doi:10.1038/ncomms13739
- 30 Dunn-Fletcher, C. E., Muglia, L. M., Pavlicev, M., Wolf, G., Sun, M. A., Hu, Y. C., . . . Muglia, L. J. (2018).
31 Anthropoid primate-specific retroviral element THE1B controls expression of CRH in placenta
32 and alters gestation length. *PLoS Biol*, 16(9), e2006337. doi:10.1371/journal.pbio.2006337
- 33 Ellison, C., & Bachtrog, D. (2019). Contingency in the convergent evolution of a regulatory network:
34 Dosage compensation in *Drosophila*. *PLoS Biol*, 17(2), e3000094.
35 doi:10.1371/journal.pbio.3000094
- 36 Ellison, C. E., & Bachtrog, D. (2013). Dosage compensation via transposable element mediated rewiring
37 of a regulatory network. *Science*, 342(6160), 846-850. doi:10.1126/science.1239552
- 38 Esnault, C., Heidmann, O., Delebecque, F., Dewannieux, M., Ribet, D., Hance, A. J., . . . Schwartz, O.
39 (2005). APOBEC3G cytidine deaminase inhibits retrotransposition of endogenous retroviruses.
40 *Nature*, 433(7024), 430-433. doi:10.1038/nature03238
- 41 Fabry, M. H., Ciabrelli, F., Munafo, M., Eastwood, E. L., Kneuss, E., Falciatori, I., . . . Czech, B. (2019).
42 piRNA-guided co-transcriptional silencing coopts nuclear export factors. *Elife*, 8.
43 doi:10.7554/eLife.47999
- 44 Feschotte, C. (2008). Transposable elements and the evolution of regulatory networks. *Nat Rev Genet*,
45 9(5), 397-405. doi:10.1038/nrg2337

- 1 Fu, Y., Kawabe, A., Etcheverry, M., Ito, T., Toyoda, A., Fujiyama, A., . . . Kakutani, T. (2013). Mobilization
2 of a plant transposon by expression of the transposon-encoded anti-silencing factor. *EMBO J*,
3 32(17), 2407-2417. doi:10.1038/emboj.2013.169
- 4 Fuentes, D. R., Swigut, T., & Wysocka, J. (2018). Systematic perturbation of retroviral LTRs reveals
5 widespread long-range effects on human gene regulation. *Elife*, 7. doi:10.7554/eLife.35989
- 6 George, J. A., Traverse, K. L., DeBaryshe, P. G., Kelley, K. J., & Pardue, M. L. (2010). Evolution of diverse
7 mechanisms for protecting chromosome ends by *Drosophila* TART telomere retrotransposons.
8 *Proc Natl Acad Sci U S A*, 107(49), 21052-21057. doi:10.1073/pnas.1015926107
- 9 Goodier, J. L., Ostertag, E. M., & Kazazian, H. H., Jr. (2000). Transduction of 3'-flanking sequences is
10 common in L1 retrotransposition. *Hum Mol Genet*, 9(4), 653-657. doi:10.1093/hmg/9.4.653
- 11 Gunawardane, L. S., Saito, K., Nishida, K. M., Miyoshi, K., Kawamura, Y., Nagami, T., . . . Siomi, M. C.
12 (2007). A slicer-mediated mechanism for repeat-associated siRNA 5' end formation in
13 *Drosophila*. *Science*, 315(5818), 1587-1590. doi:10.1126/science.1140494
- 14 Han, B. W., Wang, W., Li, C., Weng, Z., & Zamore, P. D. (2015). Noncoding RNA. piRNA-guided
15 transposon cleavage initiates Zucchini-dependent, phased piRNA production. *Science*,
16 348(6236), 817-821. doi:10.1126/science.aaa1264
- 17 Helleu, Q., & Levine, M. T. (2018). Recurrent Amplification of the Heterochromatin Protein 1 (HP1)
18 Gene Family across Diptera. *Mol Biol Evol*, 35(10), 2375-2389. doi:10.1093/molbev/msy128
- 19 Herold, A., Suyama, M., Rodrigues, J. P., Braun, I. C., Kutay, U., Carmo-Fonseca, M., . . . Izaurralde, E.
20 (2000). TAP (NXF1) belongs to a multigene family of putative RNA export factors with a
21 conserved modular architecture. *Mol Cell Biol*, 20(23), 8996-9008.
22 doi:10.1128/mcb.20.23.8996-9008.2000
- 23 Huang, W., Carbone, M. A., Magwire, M. M., Peiffer, J. A., Lyman, R. F., Stone, E. A., . . . Mackay, T. F.
24 (2015). Genetic basis of transcriptome diversity in *Drosophila melanogaster*. *Proc Natl Acad Sci*
25 *U S A*, 112(44), E6010-6019. doi:10.1073/pnas.1519159112
- 26 Huang, W., Massouras, A., Inoue, Y., Peiffer, J., Ramia, M., Tarone, A. M., . . . Mackay, T. F. (2014).
27 Natural variation in genome architecture among 205 *Drosophila melanogaster* Genetic
28 Reference Panel lines. *Genome Res*, 24(7), 1193-1208. doi:10.1101/gr.171546.113
- 29 Hur, J. K., Luo, Y., Moon, S., Ninova, M., Marinov, G. K., Chung, Y. D., & Aravin, A. A. (2016). Splicing-
30 independent loading of TREX on nascent RNA is required for efficient expression of dual-strand
31 piRNA clusters in *Drosophila*. *Genes Dev*, 30(7), 840-855. doi:10.1101/gad.276030.115
- 32 Jacobs, F. M., Greenberg, D., Nguyen, N., Haeussler, M., Ewing, A. D., Katzman, S., . . . Haussler, D.
33 (2014). An evolutionary arms race between KRAB zinc-finger genes ZNF91/93 and SVA/L1
34 retrotransposons. *Nature*, 516(7530), 242-245. doi:10.1038/nature13760
- 35 Johnson, N. R., Yeoh, J. M., Coruh, C., & Axtell, M. J. (2016). Improved Placement of Multi-mapping
36 Small RNAs. *G3 (Bethesda)*, 6(7), 2103-2111. doi:10.1534/g3.116.030452
- 37 Joly-Lopez, Z., & Bureau, T. E. (2018). Exaptation of transposable element coding sequences. *Curr Opin*
38 *Genet Dev*, 49, 34-42. doi:10.1016/j.gde.2018.02.011
- 39 Joly-Lopez, Z., Hoen, D. R., Blanchette, M., & Bureau, T. E. (2016). Phylogenetic and Genomic Analyses
40 Resolve the Origin of Important Plant Genes Derived from Transposable Elements. *Mol Biol*
41 *Evol*, 33(8), 1937-1956. doi:10.1093/molbev/msw067
- 42 Jurka, J. (2000). Repbase update: a database and an electronic journal of repetitive elements. *Trends*
43 *Genet*, 16(9), 418-420. doi:10.1016/s0168-9525(00)02093-x
- 44 Kapusta, A., Kronenberg, Z., Lynch, V. J., Zhuo, X., Ramsay, L., Bourque, G., . . . Feschotte, C. (2013).
45 Transposable elements are major contributors to the origin, diversification, and regulation of

- 1 vertebrate long noncoding RNAs. *PLoS Genet*, *9*(4), e1003470.
2 doi:10.1371/journal.pgen.1003470
- 3 Kelleher, E. S., Edelman, N. B., & Barbash, D. A. (2012). Drosophila interspecific hybrids phenocopy
4 piRNA-pathway mutants. *PLoS Biol*, *10*(11), e1001428. doi:10.1371/journal.pbio.1001428
- 5 Khurana, J. S., Xu, J., Weng, Z., & Theurkauf, W. E. (2010). Distinct functions for the Drosophila piRNA
6 pathway in genome maintenance and telomere protection. *PLoS Genet*, *6*(12), e1001246.
7 doi:10.1371/journal.pgen.1001246
- 8 Kim, D., Langmead, B., & Salzberg, S. L. (2015). HISAT: a fast spliced aligner with low memory
9 requirements. *Nat Methods*, *12*(4), 357-360. doi:10.1038/nmeth.3317
- 10 Klein, S. J., & O'Neill, R. J. (2018). Transposable elements: genome innovation, chromosome diversity,
11 and centromere conflict. *Chromosome Res*, *26*(1-2), 5-23. doi:10.1007/s10577-017-9569-5
- 12 Kolaczowski, B., Hupaló, D. N., & Kern, A. D. (2011). Recurrent adaptation in RNA interference genes
13 across the Drosophila phylogeny. *Mol Biol Evol*, *28*(2), 1033-1042. doi:10.1093/molbev/msq284
- 14 Kurtz, S., Phillippy, A., Delcher, A. L., Smoot, M., Shumway, M., Antonescu, C., & Salzberg, S. L. (2004).
15 Versatile and open software for comparing large genomes. *Genome Biol*, *5*(2), R12.
16 doi:10.1186/gb-2004-5-2-r12
- 17 Langmead, B. (2010). Aligning short sequencing reads with Bowtie. *Curr Protoc Bioinformatics*, Chapter
18 11, Unit 11 17. doi:10.1002/0471250953.bi1107s32
- 19 Langmead, B., & Salzberg, S. L. (2012). Fast gapped-read alignment with Bowtie 2. *Nat Methods*, *9*(4),
20 357-359. doi:10.1038/nmeth.1923
- 21 Lee, Y. C. (2015). The Role of piRNA-Mediated Epigenetic Silencing in the Population Dynamics of
22 Transposable Elements in Drosophila melanogaster. *PLoS Genet*, *11*(6), e1005269.
23 doi:10.1371/journal.pgen.1005269
- 24 Lee, Y. C., Leek, C., & Levine, M. T. (2017). Recurrent Innovation at Genes Required for Telomere
25 Integrity in Drosophila. *Mol Biol Evol*, *34*(2), 467-482. doi:10.1093/molbev/msw248
- 26 Lee, Y. C. G., & Karpen, G. H. (2017). Pervasive epigenetic effects of Drosophila euchromatic
27 transposable elements impact their evolution. *Elife*, *6*. doi:10.7554/eLife.25762
- 28 Levine, M. T., Vander Wende, H. M., Hsieh, E., Baker, E. P., & Malik, H. S. (2016). Recurrent Gene
29 Duplication Diversifies Genome Defense Repertoire in Drosophila. *Mol Biol Evol*, *33*(7), 1641-
30 1653. doi:10.1093/molbev/msw053
- 31 Levis, R. W., Ganesan, R., Houtchens, K., Tolar, L. A., & Sheen, F. M. (1993). Transposons in place of
32 telomeric repeats at a Drosophila telomere. *Cell*, *75*(6), 1083-1093. doi:10.1016/0092-
33 8674(93)90318-k
- 34 Li, H., Handsaker, B., Wysoker, A., Fennell, T., Ruan, J., Homer, N., . . . Genome Project Data Processing,
35 S. (2009). The Sequence Alignment/Map format and SAMtools. *Bioinformatics*, *25*(16), 2078-
36 2079. doi:10.1093/bioinformatics/btp352
- 37 Loytynoja, A. (2014). Phylogeny-aware alignment with PRANK. *Methods Mol Biol*, *1079*, 155-170.
38 doi:10.1007/978-1-62703-646-7_10
- 39 Lynch, V. J., Leclerc, R. D., May, G., & Wagner, G. P. (2011). Transposon-mediated rewiring of gene
40 regulatory networks contributed to the evolution of pregnancy in mammals. *Nat Genet*, *43*(11),
41 1154-1159. doi:10.1038/ng.917
- 42 Lynch, V. J., Nnamani, M. C., Kapusta, A., Brayer, K., Plaza, S. L., Mazur, E. C., . . . Wagner, G. P. (2015).
43 Ancient transposable elements transformed the uterine regulatory landscape and
44 transcriptome during the evolution of mammalian pregnancy. *Cell Rep*, *10*(4), 551-561.
45 doi:10.1016/j.celrep.2014.12.052

- 1 Mackay, T. F., Richards, S., Stone, E. A., Barbadilla, A., Ayroles, J. F., Zhu, D., . . . Gibbs, R. A. (2012). The
2 *Drosophila melanogaster* Genetic Reference Panel. *Nature*, *482*(7384), 173-178.
3 doi:10.1038/nature10811
- 4 Malik, H. S., Burke, W. D., & Eickbush, T. H. (1999). The age and evolution of non-LTR retrotransposable
5 elements. *Mol Biol Evol*, *16*(6), 793-805. doi:10.1093/oxfordjournals.molbev.a026164
- 6 Mari-Ordonez, A., Marchais, A., Etcheverry, M., Martin, A., Colot, V., & Voinnet, O. (2013).
7 Reconstructing de novo silencing of an active plant retrotransposon. *Nat Genet*, *45*(9), 1029-
8 1039. doi:10.1038/ng.2703
- 9 Martin, M. (2011). Cutadapt removes adapter sequences from high-throughput sequencing reads.
10 *2011*, *17*(1), 3. doi:10.14806/ej.17.1.200
- 11 McCue, A. D., Nuthikattu, S., & Slotkin, R. K. (2013). Genome-wide identification of genes regulated in
12 trans by transposable element small interfering RNAs. *RNA Biol*, *10*(8), 1379-1395.
13 doi:10.4161/rna.25555
- 14 Mohn, F., Handler, D., & Brennecke, J. (2015). Noncoding RNA. piRNA-guided slicing specifies
15 transcripts for Zucchini-dependent, phased piRNA biogenesis. *Science*, *348*(6236), 812-817.
16 doi:10.1126/science.aaa1039
- 17 Molaro, A., & Malik, H. S. (2016). Hide and seek: how chromatin-based pathways silence retroelements
18 in the mammalian germline. *Curr Opin Genet Dev*, *37*, 51-58. doi:10.1016/j.gde.2015.12.001
- 19 Moran, J. V., DeBerardinis, R. J., & Kazazian, H. H., Jr. (1999). Exon shuffling by L1 retrotransposition.
20 *Science*, *283*(5407), 1530-1534. doi:10.1126/science.283.5407.1530
- 21 Murano, K., Iwasaki, Y. W., Ishizu, H., Mashiko, A., Shibuya, A., Kondo, S., . . . Siomi, H. (2019). Nuclear
22 RNA export factor variant initiates piRNA-guided co-transcriptional silencing. *EMBO J*, *38*(17),
23 e102870. doi:10.15252/embj.2019102870
- 24 Nosaka, M., Itoh, J., Nagato, Y., Ono, A., Ishiwata, A., & Sato, Y. (2012). Role of transposon-derived
25 small RNAs in the interplay between genomes and parasitic DNA in rice. *PLoS Genet*, *8*(9),
26 e1002953. doi:10.1371/journal.pgen.1002953
- 27 Notwell, J. H., Chung, T., Heavner, W., & Bejerano, G. (2015). A family of transposable elements co-
28 opted into developmental enhancers in the mouse neocortex. *Nat Commun*, *6*, 6644.
29 doi:10.1038/ncomms7644
- 30 Obbard, D. J., Jiggins, F. M., Bradshaw, N. J., & Little, T. J. (2011). Recent and recurrent selective sweeps
31 of the antiviral RNAi gene Argonaute-2 in three species of *Drosophila*. *Mol Biol Evol*, *28*(2),
32 1043-1056. doi:10.1093/molbev/msq280
- 33 Obbard, D. J., Jiggins, F. M., Halligan, D. L., & Little, T. J. (2006). Natural selection drives extremely rapid
34 evolution in antiviral RNAi genes. *Curr Biol*, *16*(6), 580-585. doi:10.1016/j.cub.2006.01.065
- 35 Obbard, D. J., Maclennan, J., Kim, K. W., Rambaut, A., O'Grady, P. M., & Jiggins, F. M. (2012). Estimating
36 divergence dates and substitution rates in the *Drosophila* phylogeny. *Mol Biol Evol*, *29*(11),
37 3459-3473. doi:10.1093/molbev/mss150
- 38 Papadopoulos, J. S., & Agarwala, R. (2007). COBALT: constraint-based alignment tool for multiple
39 protein sequences. *Bioinformatics*, *23*(9), 1073-1079. doi:10.1093/bioinformatics/btm076
- 40 Parhad, S. S., & Theurkauf, W. E. (2019). Rapid evolution and conserved function of the piRNA
41 pathway. *Open Biol*, *9*(1), 180181. doi:10.1098/rsob.180181
- 42 Petrov, D. A., Fiston-Lavier, A. S., Lipatov, M., Lenkov, K., & Gonzalez, J. (2011). Population genomics of
43 transposable elements in *Drosophila melanogaster*. *Mol Biol Evol*, *28*(5), 1633-1644.
44 doi:10.1093/molbev/msq337

- 1 Pickeral, O. K., Makalowski, W., Boguski, M. S., & Boeke, J. D. (2000). Frequent human genomic DNA
2 transduction driven by LINE-1 retrotransposition. *Genome Res*, *10*(4), 411-415.
3 doi:10.1101/gr.10.4.411
- 4 Pontis, J., Planet, E., Offner, S., Turelli, P., Duc, J., Coudray, A., . . . Trono, D. (2019). Hominoid-Specific
5 Transposable Elements and KZFPs Facilitate Human Embryonic Genome Activation and Control
6 Transcription in Naive Human ESCs. *Cell Stem Cell*, *24*(5), 724-735 e725.
7 doi:10.1016/j.stem.2019.03.012
- 8 Quinlan, A. R., & Hall, I. M. (2010). BEDTools: a flexible suite of utilities for comparing genomic
9 features. *Bioinformatics*, *26*(6), 841-842. doi:10.1093/bioinformatics/btq033
- 10 Rahman, R., Chirn, G. W., Kanodia, A., Sytnikova, Y. A., Brembs, B., Bergman, C. M., & Lau, N. C. (2015).
11 Unique transposon landscapes are pervasive across *Drosophila melanogaster* genomes. *Nucleic
12 Acids Res*, *43*(22), 10655-10672. doi:10.1093/nar/gkv1193
- 13 Ramirez, F., Dundar, F., Diehl, S., Gruning, B. A., & Manke, T. (2014). deepTools: a flexible platform for
14 exploring deep-sequencing data. *Nucleic Acids Res*, *42*(Web Server issue), W187-191.
15 doi:10.1093/nar/gku365
- 16 Roberts, A., & Pachter, L. (2013). Streaming fragment assignment for real-time analysis of sequencing
17 experiments. *Nat Methods*, *10*(1), 71-73. doi:10.1038/nmeth.2251
- 18 Rouget, C., Papin, C., Boureux, A., Meunier, A. C., Franco, B., Robine, N., . . . Simonelig, M. (2010).
19 Maternal mRNA deadenylation and decay by the piRNA pathway in the early *Drosophila*
20 embryo. *Nature*, *467*(7319), 1128-1132. doi:10.1038/nature09465
- 21 Sackton, T. B., Kulathinal, R. J., Bergman, C. M., Quinlan, A. R., Dopman, E. B., Carneiro, M., . . . Clark, A.
22 G. (2009). Population genomic inferences from sparse high-throughput sequencing of two
23 populations of *Drosophila melanogaster*. *Genome Biol Evol*, *1*, 449-465.
24 doi:10.1093/gbe/evp048
- 25 Saint-Leandre, B., Nguyen, S. C., & Levine, M. T. (2019). Diversification and collapse of a telomere
26 elongation mechanism. *Genome Res*, *29*(6), 920-931. doi:10.1101/gr.245001.118
- 27 Satyaki, P. R., Cuykendall, T. N., Wei, K. H., Brideau, N. J., Kwak, H., Aruna, S., . . . Barbash, D. A. (2014).
28 The Hmr and Lhr hybrid incompatibility genes suppress a broad range of heterochromatic
29 repeats. *PLoS Genet*, *10*(3), e1004240. doi:10.1371/journal.pgen.1004240
- 30 Savitsky, M., Kravchuk, O., Melnikova, L., & Georgiev, P. (2002). Heterochromatin protein 1 is involved
31 in control of telomere elongation in *Drosophila melanogaster*. *Mol Cell Biol*, *22*(9), 3204-3218.
32 doi:10.1128/mcb.22.9.3204-3218.2002
- 33 Savitsky, M., Kwon, D., Georgiev, P., Kalmykova, A., & Gvozdev, V. (2006). Telomere elongation is under
34 the control of the RNAi-based mechanism in the *Drosophila* germline. *Genes Dev*, *20*(3), 345-
35 354. doi:10.1101/gad.370206
- 36 Sheen, F. M., & Levis, R. W. (1994). Transposition of the LINE-like retrotransposon TART to *Drosophila*
37 chromosome termini. *Proc Natl Acad Sci U S A*, *91*(26), 12510-12514.
38 doi:10.1073/pnas.91.26.12510
- 39 Shpiz, S., & Kalmykova, A. (2011). Role of piRNAs in the *Drosophila* telomere homeostasis. *Mob Genet
40 Elements*, *1*(4), 274-278. doi:10.4161/mge.18301
- 41 Shpiz, S., Kwon, D., Uneva, A., Kim, M., Klenov, M., Rozovsky, Y., . . . Kalmykova, A. (2007).
42 Characterization of *Drosophila* telomeric retroelement TAHRE: transcription, transpositions,
43 and RNAi-based regulation of expression. *Mol Biol Evol*, *24*(11), 2535-2545.
44 doi:10.1093/molbev/msm205

- 1 Shpiz, S., Olovnikov, I., Sergeeva, A., Lavrov, S., Abramov, Y., Savitsky, M., & Kalmykova, A. (2011).
2 Mechanism of the piRNA-mediated silencing of *Drosophila* telomeric retrotransposons. *Nucleic*
3 *Acids Res*, 39(20), 8703-8711. doi:10.1093/nar/gkr552
- 4 Simkin, A., Wong, A., Poh, Y. P., Theurkauf, W. E., & Jensen, J. D. (2013). Recurrent and recent selective
5 sweeps in the piRNA pathway. *Evolution*, 67(4), 1081-1090. doi:10.1111/evo.12011
- 6 Song, J., Liu, J., Schnakenberg, S. L., Ha, H., Xing, J., & Chen, K. C. (2014). Variation in piRNA and
7 transposable element content in strains of *Drosophila melanogaster*. *Genome Biol Evol*, 6(10),
8 2786-2798. doi:10.1093/gbe/evu217
- 9 Stamatakis, A. (2014). RAxML version 8: a tool for phylogenetic analysis and post-analysis of large
10 phylogenies. *Bioinformatics*, 30(9), 1312-1313. doi:10.1093/bioinformatics/btu033
- 11 Thomas, J. H., & Schneider, S. (2011). Coevolution of retroelements and tandem zinc finger genes.
12 *Genome Res*, 21(11), 1800-1812. doi:10.1101/gr.121749.111
- 13 Thurmond, J., Goodman, J. L., Strelets, V. B., Attrill, H., Gramates, L. S., Marygold, S. J., . . . FlyBase, C.
14 (2019). FlyBase 2.0: the next generation. *Nucleic Acids Res*, 47(D1), D759-D765.
15 doi:10.1093/nar/gky1003
- 16 Traverse, K. L., & Pardue, M. L. (1988). A spontaneously opened ring chromosome of *Drosophila*
17 *melanogaster* has acquired He-T DNA sequences at both new telomeres. *Proc Natl Acad Sci U S*
18 *A*, 85(21), 8116-8120. doi:10.1073/pnas.85.21.8116
- 19 Villasante, A., Abad, J. P., Planello, R., Mendez-Lago, M., Celniker, S. E., & de Pablos, B. (2007).
20 *Drosophila* telomeric retrotransposons derived from an ancestral element that was recruited to
21 replace telomerase. *Genome Res*, 17(12), 1909-1918. doi:10.1101/gr.6365107
- 22 Volff, J. N. (2006). Turning junk into gold: domestication of transposable elements and the creation of
23 new genes in eukaryotes. *Bioessays*, 28(9), 913-922. doi:10.1002/bies.20452
- 24 Walter, M. F., Biessmann, M. R., Benitez, C., Torok, T., Mason, J. M., & Biessmann, H. (2007). Effects of
25 telomere length in *Drosophila melanogaster* on life span, fecundity, and fertility. *Chromosoma*,
26 116(1), 41-51. doi:10.1007/s00412-006-0081-5
- 27 Wang, L., Barbash, D. A., & Kelleher, E. S. (2019). Divergence of piRNA pathway proteins affects piRNA
28 biogenesis and off-target effects, but not TE transcripts, revealing a hidden robustness to piRNA
29 silencing. *bioRxiv*.
- 30 Wang, L., Dou, K., Moon, S., Tan, F. J., & Zhang, Z. Z. (2018). Hijacking Oogenesis Enables Massive
31 Propagation of LINE and Retroviral Transposons. *Cell*, 174(5), 1082-1094 e1012.
32 doi:10.1016/j.cell.2018.06.040
- 33 Wang, W., Yoshikawa, M., Han, B. W., Izumi, N., Tomari, Y., Weng, Z., & Zamore, P. D. (2014). The initial
34 uridine of primary piRNAs does not create the tenth adenine that is the hallmark of secondary
35 piRNAs. *Mol Cell*, 56(5), 708-716. doi:10.1016/j.molcel.2014.10.016
- 36 Waterhouse, A. M., Procter, J. B., Martin, D. M., Clamp, M., & Barton, G. J. (2009). Jalview Version 2--a
37 multiple sequence alignment editor and analysis workbench. *Bioinformatics*, 25(9), 1189-1191.
38 doi:10.1093/bioinformatics/btp033
- 39 Wei, K. H., Reddy, H. M., Rathnam, C., Lee, J., Lin, D., Ji, S., . . . Barbash, D. A. (2017). A Pooled
40 Sequencing Approach Identifies a Candidate Meiotic Driver in *Drosophila*. *Genetics*, 206(1), 451-
41 465. doi:10.1534/genetics.116.197335
- 42 Wintersinger, J. A., & Wasmuth, J. D. (2015). Kablammo: an interactive, web-based BLAST results
43 visualizer. *Bioinformatics*, 31(8), 1305-1306. doi:10.1093/bioinformatics/btu808
- 44 Zhao, K., Cheng, S., Miao, N., Xu, P., Lu, X., Zhang, Y., . . . Yu, Y. (2019). A Pandal complex adapted for
45 piRNA-guided transposon silencing. *bioRxiv*.
46